II. BATTERIES AND FUEL CELLS

Harvey J. Schwartz, J. Stewart Fordyce, Robert B. King, James M. McKee,
Daniel G. Soltis, and Lawrence H. Thaller

INTRODUCTION

Since electrochemical systems will be used for a long time to come, it is worthwhile to discuss briefly what might be gained by improving these systems. First, consider the battery which is the main energy storage and conversion device in use today. One obvious area for improvement is in energy density, or the watt-hours of energy delivered per pound of battery weight. The silver-zinc primary battery, the main one used today, delivers from 30 to 90 watt-hours per pound depending on its discharge rate. This means that approximately 10 to 35 pounds of batteries must be supplied for each kilowatt-hour delivered. The situation is even worse for secondary or rechargeable cells. For this type of service the silver-zinc battery can not be used because of a variety of problems which will be discussed later. Therefore, the less energetic silver-cadmium and nickel-cadmium systems must be used. These have good cycle life, but the silver-cadmium cells are restricted to use in situations where low charge rates are acceptable. This leaves nickel-cadmium as the only proven, reliable battery system for long-term service where rapid recharge is needed, such as for low-altitude Earth-orbiting satellites. However, the nickel-cadmium cell only delivers a few watt-hours per pound, if long life is desired. It is apparent why this causes concern if one considers the 50-kilowatt solar-cell power system using nickel-cadmium batteries for energy storage. If lifetimes of several years are necessary, approximately 15 000 pounds of batteries would be required if a rather optimistic 2 watt-hours per pound were assigned as the energy density of the battery. It is obvious that 5000 pounds could be saved if the energy density delivered were 3 instead of 2 watt-hours per pound. Since expected cost per pound of material in orbit is roughly equivalent to its weight in gold (i.e., $500/lb), this would represent a tangible "savings" of $250 000 per application. Improving the energy density from 2 to 3 watt-hours per pound sounds easy, until one realizes that a number of years of research have not significantly increased the energy density of this system, and that at present, the mechanism of the reaction occurring at the nickel electrode is not known for certain.

It can be seen that much can be gained from improving energy density. Similar arguments can be made for improving other parameters, such as life, temperature capability, reliability, etc., for fuel cells as well as batteries. Our electrochemical technology program, which is aimed at improving the performance of all types of electrochemical systems, is divided into the following four areas:

(1) Work on conventional batteries, such as nickel-cadmium or silver-zinc

(2) Improvement in battery performance at extreme temperatures, both high and low

(3) Research on new systems that promise major increases in energy density

(4) Research and development on fuel cell systems and components of all types

Approximately 80 percent of the NASA spacecraft flown to date have carried nickel-cadmium secondary batteries. As noted previously, this nickel-cadmium system is characterized by long-life operation and unfortunately by low energy density where long service is required. Work on the nickel-cadmium system is an important part of the conventional battery improvement program.

STABILITY AND STRUCTURE OF NICKEL OXIDES

One way of improving performance of existing systems is to increase the efficiency of the reactants. In the nickel-cadmium system, one of the persistent problems is the loss of charge on the nickel oxide electrode on standing at open circuit. The mechanism for the loss of charge has been studied comprehensively by Conway and Bourgault (ref. 1) who concluded that the reaction is controlled by the electrochemical reaction of oxygen evolution, rather than the nonelectrochemical decomposition or oxygen desorption from the surface phase which had been advanced by others (ref. 2). The details of the mechanism are still not completely resolved. The technological problem remains, however, and work is being supported at Gulton Industries, Inc. to look into ways of stabilizing the charged electrode especially at elevated temperature where the loss of charge is severe. This is needed because the battery must perform under a variety of ambient conditions for space application. Two approaches have been taken so far. One is to charge the electrode at different rates and temperatures to study the influence of these variables on the stand characteristics. No really significant improvements have been obtained in this way. A second approach has been to introduce cations other than nickel into the electrode. The transition metal ions such as cobalt and manganese introduced at a level of 20 atom percent were found to have a marked improvement on retention characteristics as shown in figure II-1 where a comparison of percent charge retention is plotted against time in days on stand at 150° F. The electrodes used for these studies were loaded with the same total number of metal ions in each case. The upper curve is for electrodes containing 20 atom percent of cobalt or manganese and 80 percent nickel, while the lower curve is for 100 percent nickel. When metals of groups I and II of the periodic table were added, inferior results to the control positives were obtained. The change in the rate of charge loss after 1 day implies a change in the mechanism which is not understood at this time. The forming process used in the electrode preparation suggests that in the case of the manganese and cobalt doped system the charged electrode consists of the mixed oxides (or hydroxides) though this has not been proven or even examined. It should be noted that the divalent cobalt and manganese hydroxides have a structure identical to the nickel compound but with slightly larger lattice dimensions. The retention results suggest that the charged cobalt and manganese oxides are stable in contrast to the nickel oxide under these conditions, though this does not account for the whole effect. Nothing is known at present how much of the electrode capacity is due to the electrochemical reduction of cobalt or manganese oxides (or hydroxides) or in what form they exist. One further point should be made that even though the mixed oxide of magnanese with

nickel imparts the same improved retention characteristics as the cobalt-nickel system there is a significant difference in the utilization efficiency in the two cases (ref. 3). This is shown in figure II-2 where the utilization efficiency (based on the capacity obtained for 100-mA discharge) is plotted against the discharge current in milliamperes. The dip in all the curves at 500 milliamperes is a real effect but is not yet explained. The manganese doped material follows the pure nickel control while the cobalt doped electrode shows enhanced utilization at all currents studied. This possibly indicates a preferred crystallite size for the mixed cobalt-nickel oxide system though this is by no means the only explanation. Much work remains to be done in this promising area.

In addition to the use of empirical methods such as those just described to improve stability, it is important to understand what occurs in the nickel oxide electrode on charging and to determine, if possible, the nature of the "charged state." Such studies provide a fundamental basis for potential improvements which are not even recognized yet. The identification and characterization of materials formed in the nickel oxide electrode at various states of charge have been the subject of much study with conflicting results (e.g., refs. 4 and 5). In view of this, the program with Gulton Industries also includes a substantial effort aimed at the ellucidation of the structure of the nickel oxide in the sintered nickel plate electrode. The X-ray diffraction technique has been employed on wet plates and good diffraction data have now been obtained (ref. 6). Figure II-3 shows the diffraction intensity as a function of diffracting angle for plates charged to the level shown. The pattern of the discharged material at the top shows the three principal reflections at 38.3°, 32.8°, and 19°. These peaks are identified by their Miller indices, 101 - 002, 100 and 001, which describe the crystallographic planes. This material is nickel hydroxide ($Ni(OH)_2$), which agrees with the conclusions of previous studies (ref. 7). As the charging level increases, there is essentially no major change in the diffraction pattern, and therefore, no change in structure occurs up to the 90-percent level. During the charging process, the active material is oxidized from Ni(II) to Ni(III) though Labat (ref. 5) has found magnetic evidence for the initial formation of Ni(IV). There is the simultaneous loss of a proton to the electrolyte solution. At 100-percent charge, the intensity of the 100 and 101 - 002 reflections begin to decrease. At 133-percent charge, the 100 reflection has completely disappeared and the 101 - 002 reflection is considerably reduced in intensity. These results, together with Kober's (ref. 7) infrared absorption data which show the formation of hydrogen bonds in the charged material relative to the discharged material where "free OH" exists, lead to the following description of the charging process. In figure II-4(a) is the unit cell of the hexagonal layer structure of nickel hydroxide ($Ni(OH)_2$) showing the positions of the nickel, oxygen, and hydrogen atoms; the presence of free OH in the structure should also be noted. This is the discharged state. Up to 90 percent of charge, the only change that occurs is the loss of one of the protons and the formation of a hydrogen bond between the two oxygens as shown in figure II-4(b). As charging continues above the 90-percent level, the intensity data indicate (by comparison with calculated intensities based on postulated structures) that the ordered layer structure disappears and is replaced by a random stacking of the layers (ref. 8).

When charge input is twice the capacity, that is, at 200-percent charge, the intensity of all the reflections is very weak, which indicates that the material is amorphous in character but another phase is making its appearance at 12.7°. As charging continues, recrystallzation to the

characteristic γ-NiOOH has occurred showing peaks at 37.5^{o}, 25.5^{o}, and 12.7^{o}. The structure of this latter material is not known but is undergoing further investigation.

The success with these studies demonstrates the feasibility of using the diffraction pattern and its intensity as a means of characterizing a charged electrode and providing insight into the process involved in its operation. The application of these and other structural tools to electrochemical problems is a fertile field for further investigation.

IMPROVED SILVER-ZINC SECONDARY CELL

The nickel-cadmium cell because of its long cycle life and performance characteristics justifies considerable effort, but a secondary system that appears very attractive on the basis of energy density is the silver-zinc couple. A couple of this type would be most desirable as a long-life secondary cell. However, due to a number of problems, its usefulness is limited to short-term applications. A number of the problems which plague this cell are the following:

(1) Soluble electrodes - silver oxide in charged state, zinc oxide in discharged state

(2) Separators not inert to their environment

(3) Zinc electrode susceptible to dendritic growth

These factors cause the cell to be limited in cycle capability. Elimination of all or some of these problems should give a cell which would find considerable use.

As a result of one of the contracts in which an attempt was made to develop an inorganic ion exchange membrane for a fuel cell, it was suggested that a similar type membrane, stable in potassium hydroxide (KOH) and of controlled pore size, could perform effectively as a separator in a secondary battery. Therefore, Astropower Laboratory of Douglas Aircraft began work to develop a membrane of this type. As a result of their investigations, a separator was developed that was inert in caustic, resisted the dendritic growth of the zinc electrode, and blocked the migration of the dissolved electrode materials. These factors alone warranted the development of this cell type. The separator is made from a combination of inorganic materials which after ball milling are compacted in the die shown in figure II-5 and then sintered. If the proper choice of materials and processing conditions is made, a controlled pore size membrane can be fabricated which will exclude the dissolved electrode materials.

The charge-discharge curves shown in figure II-6 are of a simple two plate cell that was tested during the feasibility study of the separator. This cell, which is one of the cells that indicated the potential of this development, was discharged at 77^{o} F at 20 milliamperes per square centimeter for 30 minutes and charged at 12 milliamperes per square centimeter for 1 hour. The voltage curves of the discharge periods were quite constant throughout the cell's life. The test was discontinued at 2700 cycles because of the degradation of the zinc electrode. In fact, most of the problems encountered in these cells were due to poor seals and failure of the zinc electrode.

Another factor which evolved during testing was the ability of this cell to operate over a wide temperature range and to withstand sterilization temperatures with little or no degradation of capacity. Figure II-7 compares the performance of two cells cycled at 77^{o} F on the 1/2-hour-charge, 1/2-hour-discharge cycle. Illustrated are cycles 1 and 220 of a sterilized and an unsterilized cell. The sterilized cell had been subjected to three periods of 36 hours each at 293^{o} F

prior to testing at 77° F. As can be seen, the performance of the cells compares favorably.

The next series of figures illustrates the cycling capability of the various cell types against temperature. Figure II-8 compares the standard silver-zinc cell against the experimental cell. The maximum cycle life of the standard cell is about 400 cycles compared to 1800 for the experimental, while the best obtained from this cell is 2700 cycles. The temperature range at which the experimental cell will operate is twice that of the standard cell (from approx. 30° to 300° F), and as can be seen, over 1000 cycles can be obtained over most of this range of temperature. These performance characteristics are a significant improvement over the state of the art. Figure II-9 shows how this performance measures up to the other systems. The nickel-cadmium cell undoubtedly has the best cycle life, but just as the other standard cells, it is limited as to the range of temperatures over which it can operate. The experimental silver-zinc cell, however, almost equals silver-cadmium performance and exceeds it considerably in respect to its operating temperature range. It is realized that the performance characteristics of all cell types are continually increasing; however, it is felt that the performance of the experimental silver-zinc cell will keep pace with these improvements and has a chance of exceeding them.

The development of the cell has progressed satisfactorily over the past 2 years and now a 9-plate, 5-ampere-hour cell is being fabricated. The construction of this cell differs somewhat from conventional types. Figure II-10 shows the basic assembly of the cell. The difference in the construction is the method in which the cell pack is assembled prior to insertion into the case. Each separator is sealed into the slotted frame to form discrete compartments, and then the electrodes are placed into these cavities. A complete seal is necessary to prevent species migration around the edge of the separator. The frame approach also facilitates assembly of the cell pack and insertion into the case. Electrolyte is added after the pack is inserted and the top seal closure made. The evaluation of these 5-ampere-hour cells has just begun.

The energy density expected from the cell should not differ significantly from standard silver-zinc cells; however, when compared with cycle life, there should be a significant difference in performance at each rate. A small weight penalty may occur because of the separator and frame construction, but other methods of encapsulation of the separator may bring this in line. In figure II-11 a comparison is made between the energy density and cycle life of the various systems. If long cycle life at low energy densities is desired, the nickel-cadmium battery should be used since as many as 10 000 cycles are reported. For shorter periods, however, the experimental silver-zinc cell would provide increased performance up to 3000 cycles. The curve for the silver-zinc cell shows a range of values with the uppermost line representing the best numbers obtained to date; the lower curve gives the average value. There is a significant difference when comparing the various cells at the higher rates for short times where on the basis of energy density the experimental silver-zinc cell exceeds them all. Any improvement in cycle life will only increase the advantages and subsequent utility of this development. Results of testing to date indicate that very few failures occur because of the separator; the major limiting aspect of this cell is the performance of the zinc electrode. A program has just been initiated to investigate what can be done to increase the efficiency and performance of this electrode. Any improvement here will surely increase the importance of this cell.

EXTREME TEMPERATURE BATTERIES

So far the discussion has been concerned with batteries that operate over the rather nominal temperature range of 0^{o} to 300^{o} F. In the space program, there are more severe operating conditions, and the nonaqueous systems for operation at extreme temperatures are being investigated. For the exploration of the surfaces of Mercury, Venus, and Mars and the possibility of close-in solar probes, a temperature range of -400^{o} to 1000^{o} F can be anticipated.

Figure II-12 illustrates the effect on battery capacity when operation is required outside of their normal temperature range. The batteries concerned are low-rate silver-zinc primary cells that were stored for 2 weeks at different test temperatures and then discharged while still at these temperatures. The percent of original capacity is plotted as a function of test temperature. Note that over the range of 0^{o} to 80^{o} F the 2-week wet stand does not reduce capacity significantly, but that at high and low temperatures the drop off is appreciably. At lower temperatures the fall off is due to poor utilization, while at elevated temperatures the phenomenon responsible is consumption of the active material due to direct chemical reaction.

There are two methods to cope with the problem of extreme thermal environments. The first is to protect the battery by thermal insulation and auxiliary heating in cold environments. The second, and preferred, is to build a battery system that will operate in the particular environment of interest.

The task of finding electrochemical systems that will operate at extreme temperatures is quite interesting. No longer will aqueous electrolytes be useful. It has been known for many years that molten mixtures of alkali halides are, in themselves, ideal nonaqueous electrolytes. They are very fluid, have high decomposition potentials, have conductivities much higher than any aqueous system, and are powerful solvents for almost any type of compound. However, the high melting points of even the eutectic mixtures of these compounds have prevented the widespread usage of this type of electrolyte.

Strangely enough there is one class of batteries which takes advantage of this fact. When batteries are made with these high-temperature electrolytes, they have literally years of room temperature shelf life, since the rates of self discharge at these temperatures are almost zero. When one wants to use these batteries one just melts the electrolyte and the battery is then ready. These cells or batteries, as the case may be, are used exclusively by the military and are referred to as thermally activated cells or simply thermal cells. In figure II-13 is a typical thermal battery.

The individual components of each cell have a layered arrangement. Calcium is usually employed as the anode. It reacts chemically with the melted electrolyte to form a liquid alloy of lithium and calcium at the anode surface. This makes an ideal electrode for high rates of discharge. The eutectic mixture of lithium chloride and potassium chloride is the usual electrolyte. A frequently employed cathode material is potassium chromate. The individual cells of the battery are brought up to the operating temperature by a pyrotechnic device that is interleaved between the individual cells. An electric match initiates the very rapid but almost gasless heat-producing chemical reaction that takes place in these layers. Thermal insulation helps keep down the heat losses from the activated battery. Because of the high solubilities of the cathode materials in the electrolyte, the rates of internal chemical reaction are very high. For this

reason, these cells can only operate a few minutes at the most. For their particular application, however, they can perform the job better than any other battery.

A few years ago NASA Lewis Research Center became interested in batteries that would operate for periods of several days at temperatures of about 800° F. One possible use would be for probes sent to the planet Venus where the surface temperatures are expected to be in that vicinity. In this application, internal heating devices to activate the battery are not too great a concern. A research program was started at Lewis to investigate possible electrochemical systems which might be useful for this application. The magnesium - copper oxide system was finally selected for intensive investigation. Figure II-14 illustrates one of several types of cells used in these studies. As to size, the cylindrical case has the same dimensions as a flashlight D cell. The copper can itself is the current collector for the cathode, and a stainless-steel shaft threaded into the anode conducts the current up through the insulated feedthrough. A woven glass separator material is employed in these cells.

The eutectic mixture of lithium chloride potassium chloride was picked for the electrolyte. It has a convenient melting point of 685° F, a high decomposition potential of about 3.5 volts, and an excellent ionic conductivity. Once the electrolyte had been picked, the electrode materials were selected on the basis of thermodynamic compatibility with it. Magnesium and cupric oxide both have high half-cell potentials, low equivalent weights, and were thought to have tolerable solubilities in the molten salt electrolyte. These hermetically sealed cells are placed in a furnace and discharged at a constant load. A typical discharge curve of this type of cell is shown in figure II-15. Here, the current, voltage of the cell under load, and the periodically observed open circuit voltage are plotted as functions of time. Two aspects of this plot are to be noted - one being the rather flat current against time curve at these light discharge rates, and the other the large step in the open circuit voltage curve. This large step is due to a change in the electrochemical reaction during the latter part of the discharge.

One of the important features being investigated in these studies is the average rate of self-discharge of different types of cell configurations. When five identical cells were discharged at different average currents and the anode efficiencies were plotted against these currents, it was found that although the anode efficiency increases with increasing current drains, the rates of self-discharge for all of these cells are about the same. From other preliminary experiments, it was deduced that this rate was controlled by the rate of diffusion of ions from the vicinity of the cathode to the anode. When cells were made that would hinder this diffusion, cells with lower rates resulted. Figure II-16 shows the value of the self-discharge rates for different cell configurations. It is seen that average rates decreased from about 200 to about 3 milliamperes as the distance was increased between the anode and cathode and other structural arrangements were made to decrease the surface area of the electrodes. The internal resistance of the cells with very high self-discharge rates is about 0.1 ohm, while for the cells with very low rates the resistance goes up to about 1 or 2 ohms. It is obvious that these latter cells cannot deliver currents as high as the former type. So it is seen that, as stated earlier, every cell made is a compromise between having low self-discharge characteristics and having the ability to deliver high current. However, from the results of these studies it will be possible to design cells which, for a given desired service life, will have the optimum balance of these two factors. The encouraging

results obtained thus far have prompted the NASA to award a contract to further study the magnesium - copper oxide system.

The next type of battery to be discussed would be useful at very low temperatures. These might be used on probes to cold environments such as the surface of Mars. Here again a nonaqueous electrolyte is called upon. These batteries, now under investigation, utilize liquid ammonia solutions as the electrolyte. The ground work for these low-temperature batteries was started some 20 years ago with what are referred to as the ammonia vapor batteries. Later with the introduction of stronger battery casings, higher vapor pressure cells offering higher performance were introduced. These higher vapor pressure cells also extended the range of low-temperature operation. Figure II-17 shows an up-to-date high pressure cell. As with the ammonia vapor cells, it is a reserve-type battery, which is one that is activated just before it is to be used. In this instance, the ammonia is contained in a reservoir above the battery section. Upon mechanical or electrical ignition of the percusion cap, the resulting pressure buildup drives the lance through the thin membrane located directly above the central ammonia manifold. The collapsing reservoir walls force the liquid into the manifold and on into the individual cell sections. The battery is now ready to deliver power. The technique of adding the electrolyte at the last minute is a common one used to bypass the problem of high self-discharge rates. The anode material is magnesium which has been plated onto silver foil; the solute for the electrolyte is potassium thiocynate; and the cathode material is metadinitrobenzene. The wide operating range of -65° to 160° F results from the use of liquid ammonia in a strong battery case.

A study was initiated by the NASA to investigate batteries for use at about -130° F. These batteries are based on the general principles of the conventional high pressure ammonia cells just discussed and, in many respects, are similar. The first area that needed investigation was that of finding whether the potassium thiocynate salt would depress the freezing point of the solution to the temperature of interest, and still serve as a suitable electrolyte. Figure II-18 shows the results of this investigation. It was found that the oxidizing agent used in the high temperature ammonia batteries was unsuitable for these low-temperature cells. Presently, mixtures of sulfur and mercuric sulfate are being investigated as the cathode materials. Concurrent with this is a study of different amounts of conductive additives for the cathode mix and their effect on the overall cell performance.

Specific requirements of the contract are for single cells that will operate for at least 3 days at a temperature of -130° F. Figure II-19 shows the discharge curve of one of these experimental cells. This particular cell had a bobbin-type construction and is characterized by a rather large drop in voltage during the first few hours of operation, followed by a gradual rise, and finally, the normal dropoff to the cutoff voltage of 1.35 volts. This large decrease in voltage at the start of operation is probably due to a change in the electrochemical mechanism at the cathode. The number of chemical and electrochemical reactions that can take place in this system is rather large and not too well understood as yet.

HIGH ENERGY DENSITY BATTERIES

Since the discussion on extreme temperature batteries is complete, attention can now be

turned to nonaqueous batteries of a different type which offer promise of major increases in energy density. It is easy to select combinations of reactants which have theoretical performance outputs that far exceed those in use today. One has only to go to the periodic table and pick the light metals on one hand as anodes and the halogens, or their compounds, on the other as cathodes. Simple free energy calculations (see table II-1) show that these are good choices. Note that the voltages for lithium anode combinations are above 3.0 volts, and that theoretical energy densities of between 500 and 750 watt-hours per pound are predicted. The magnesium-ACL system is of interest in the dry tape battery, which will be described later. While organic compounds tend to be heavy cathodes, the ACL shown here is representative of a promising class of compounds that are characterized by complex structures containing multiple positive chlorine atoms.

As attractive as these figures are, the materials are comparatively expensive and no large-scale commercial market has been evident, so that work, mainly under government support, on these systems has essentially started from scratch in recent years.

Once promising electrode couples have been chosen from the periodic table, the next problem to be faced is the selection of an appropriate electrolyte. The electrolyte in any dynamic electrochemical system is required to ensure charge neutralization at the electrode surfaces by giving or taking ions from the interfaces as electrons flow in the external circuit. It also completes the electrical circuit (as you have heard) and contributes a series resistance which conducts by the migration of ions in the potential gradient across the cell. These functions involve mass transport processes and are influenced by the physical properties such as the viscosity of the medium in which they occur.

For best performance, a battery electrolyte must have the following general properties:

(1) Good stability - It must not react chemically or electrochemically with the electrode materials or decompose under the conditions of operation.

(2) Good conductivity - It must permit reasonable current drain without excessive ohmic drop. Since they are ionic conductors, this implies the presence of a sufficient number of ions with adequate mobility.

(3) Low viscosity - This is desirable to maximize the diffusion of the reactants or products of the electrochemical reaction to or from the vicinity of the electrodes. If the rate of diffusion is slow compared to the rate of electrochemical reaction, severe concentration gradients can form. This leads to a decrease in the cell potential, the so-called concentration polarization, which is to be avoided wherever possible.

Now to the problem in a high energy density battery. First of all, since active metal anodes such as lithium are being used, any electrolyte containing water is ruled out since rapid reaction may occur with these metals to liberate hydrogen gas. One must go then to the so-called nonaqueous solutions, which in the moderate temperature range are based on organic materials as solvents for the most part. Of these materials, those which react readily with the active metals must be avoided of course. The most critical requirement, though, is the need to provide good conductivity. This implies that the organic solvent must be capable of dissolving ionic solids to form ions in solution. To guide the selection from among the many organic solvents, those properties of a solvent are considered that influence its ability to dissolve ionic solids to form a useful electrolyte system.

In order for an ionic solid to dissolve in any solvent, the ions in solution must represent a more stable state than the ions in the solid lattice. The magnitude of the difference in stability of these two states of the system will determine the extent of the solubility. (The process is described in fig. II-20.) For ionic solids, the lattice is held intact by strong forces; the energy needed to dissociate the solid to its ions is referred to as the lattice energy and is defined in such a way that the greater the lattice energy the more stable the solid. When ions go into solution, they combine with the solvent to form so-called solvated ions. These are ions that are tightly bound to one or more molecules of solvent. The energy liberated in this process, the so-called solvation energy, is defined in such a way that the greater the solvation energy the greater the stability of the solvated ions. If the solvation energy exceeds the lattice energy, then the solid will go into solution since this will be the most stable state of the system.

Most organic solvents have a handicap with regard to their solvation properties because those able to do so will solvate the positively charged cations to a greater extent than the negatively charged anions which are hardly solvated at all. This contrasts with the situation in water where both anions like the chloride ion and cations like the sodium ion are solvated to roughly the same extent. Since the solvation of both anions and cations contributes to the solvation energy leading to solution of the solid, the inability of the anion to contribute very much in the organic solvent leads to a lower solubility than in water for those solids with large lattice energies (ref. 9). The only way to overcome this handicap is to use solvents having very large ion solvation energies. Large solvation energies are associated with those molecules which are polar, that is, those which possess separated centers of positive and negative charge. This requirement is most stringent in the high energy density program since lithium anodes are being used and solvents are needed which will dissolve lithium salts, in particular the halides. These have large lattice energies because of the small size of the lithium ion.

It is indeed possible to find appropriate polar solvents to dissolve ionic solids of interest. However, it should be emphasized that even in dilute solution it is possible that the ions are not "free" but are associated by electrostatic forces to form nonconducting ion pairs in solution, as illustrated in figure II-21; thus, even though solubility has been achieved, conductance may be impaired. The extent of ion pair formation is a sensitive function of the dielectric constant of the solvent. The laws of electrostatics would predict that the force holding such an ion pair together is greater the lower the dielectric constant of the medium. Thus, the equilibrium shifts to the right in media of low dielectric constant and vice-versa. In figure II-22 are experimental results illustrating this (ref. 10), where the equilibrium constants for the formation of a typical ion pair are plotted as functions of the dielectric constant. It is noted that for this particular system the extent of ion pair formation drops rapidly and becomes negligible at a dielectric constant of 44 or a log of 1.63. In this case the ions involved (tetraisoamylammonium nitrate) are quite large, and the ion pair is unstable at this value of the dielectric constant. For smaller ions, an even larger dielectric constant is needed to prevent significant ion pair formation. This is a classic experiment which illustrates very well the advantage of high dielectric constant media to enhance conductivity. Though this simple consideration applies only in dilute solutions, it can be explained quantitatively by the electrostatic theory of ion pair formation developed by Bjerrum which provides the solid line through the points. The electrostatic aspects are only part of the picture, however; in any system of practical significance where high concentrations are en-

countered, many complex interactions involving both chemical and physical effects can occur.

The third requirement of a battery electrolyte, namely low viscosity, has to be considered. As far as the solvents are concerned, this means that the molecules should be symmetric and of relatively small size. However, the addition of a solute can drastically modify the structure of a liquid and change its properties. These influences must be kept in mind.

On the basis of the foregoing considerations, namely large ion solvation energy, high dielectric constant, which is typically in the range from 35 to 65 compared to water with a value of 80, and low viscosity, nonaqueous solvents that will all dissolve ionic solids to form electrolytes of value in high energy density systems can be selected. Some of these nonaqueous solvents, their abbreviations, and dielectric constants are as follows:

N-nitroso-dimethylamine	NDA	53
Methyl formate	MF	8.5
Dimethyl sulfoxide	DMSO	46
Acetonitrile	AN	37
Dimethyl formamide	DMF	37
Propylene carbonate	PC	64
γ-Butyrolactone	BL	39

Methyl formate though a suitable solvent is anomolous in that it has a dielectric constant of only 8.5. It serves to emphasize the importance of other factors.

Since the conductivity of the electrolyte must be as large as possible for battery application, it is instructive to examine the conductance, as a function of the concentration of solute over a wide range. In figure II-23 (ref. 11) are conductance-concentration plots for a couple of electrolytes in dimethyl formamide to show typical behavior. The increase in conductivity with larger ion size should be noted. The curves show a maximum value at approximately 1.5 molal concentration, which is typical for nonaqueous systems. This may result from either ion pairing or from the pronounced increase in viscosity of DMF containing high concentrations of salts. Remember that conductivity involves mass transport and is sensitive to any property which impedes ion movement.

For the case of KPF_6, it is probable that the appearance of a maximum in the conductivity curve is predominantly due to the viscosity increase, not to ion pair formation. This is shown in figure II-24 where the viscosity and conductance are plotted together. The increase in viscosity coincides approximately with the drop in conductance. This may be a typical phenomenon in these types of concentrated electrolytes though the absence of quantitative data of this kind for practical systems makes it difficult to deduce what limitations are being imposed by nature in any given situation.

These limitations, which are rather specific for nonaqueous electrolytes, do have implications in the optimum design of high energy density batteries. As an example, a system is considered in which the products of the electrochemical discharge are soluble. To minimize the ohmic drop, it would be logical to choose an electrolyte concentration to provide maximum conductivity. As the cell discharges, there would be a pronounced increase in the electrolyte concentration since the amount of solution in the battery is minimized to achieve the highest energy

density. Because of this, the conductivity decreases and the viscosity increases. As a consequence, the cell potential drops for two reasons: increased ohmic resistance, and concentration polarization caused by the mass transport restrictions. As a trade off in actual battery design, it is desirable to start with an electrolyte concentration somewhere below that for maximum conductivity to achieve more uniform operating characteristics.

It is felt that if the limitations in nonaqueous electrolytes are identified and understood, then guidelines can be provided which will allow their influence to be reduced or avoided entirely. NASA and other agencies are funding programs to provide this insight.

Since theoretical considerations have been taken into account, some typical conductivity data will be examined. Table II 2 compares the conductivity of three popular electrolytes, one aqueous and two nonaqueous. If water is the solvent, potassium hydroxide (KOH) gives a maximum conductivity of 55×10^{-2} ohm^{-1} centimeter^{-1}; $LiClO_4$ with methyl formate gives 2.6×10^{-2} ohm^{-1} centimeter^{-1} while with propylene carbonate, this is reduced to 0.5×10^{-2}. Note that the conductivity of the aqueous KOH electrolyte is over one order of magnitude greater than the MF system and two orders of magnitude greater than the PC system. Obviously, it would be desirable to use the aqueous KOH electrolyte, but a lithium anode reacts violently with it. It also reacts slowly with MF. Of the systems shown, only the PC electrolyte is stable. Table II-3 demonstrates the ohmic losses due to electrolyte resistance for the materials shown in table II-2 for an electrode spacing of 1 millimeter. For KOH in H_2O, the voltage loss at a current density of 10 milliamperes per square centimeter is about 0.002 volt. For $LiClO_4$ in MF, the loss is 0.0385 volt, and for $LiClO_4$ in PC, it is 0.2 volt. If the last system should operate at 100 milliamperes per square centimeter, it would suffer an ohmic loss of 2 volts, which would be an unacceptably high loss in performance.

From the previous discussion it is obvious that conductance alone is not a satisfactory basis for choosing an electrolyte. Sometimes trace amounts of materials apparently affect electrolyte properties. Figure II-25 demonstrates what may happen when a substance dissolves in a nonaqueous solvent. At the top of the figure is shown a cation, or positively charged ion, being solvated by a pure nonaqueous solvent. If a trace of water is present, it is seen that the cation may be preferentially solvated by the water. Both species, as well as intermediate forms, probably exist in the solution. In any case, the solvation energies will be different and will thus shift the position of any equilibria involved. Figure II-26 shows the effect of a trace amount of an unknown impurity upon a lithium anode performance. A technique called preelectrolysis, which involves passing a small current through the cell, was used to remove certain impurities from the electrolyte. Before preelectrolysis, the efficiencies are quite low. After overnight preelectrolysis, which apparently removed the unknown material, the efficiencies are dramatically improved. Note that before preelectrolysis, zero efficiency was obtained up to about 12 milliamperes per square centimeter. Apparently reduction of the impurity consumed the current instead of the desired process, reduction of Li^+ to Li^0 metal. Trace amounts of materials may be in the material as received or they may be accidentally added. Two cases of the latter may be cited from experience. In one case, traces of water were introduced by using presumably pure argon as an inert atmosphere. In a second case, foreign ions were introduced from a desiccant used to remove water. It is only fair, however, to note that trace amounts of certain materials may be necessary for satisfactory cell operation. It is felt that the solution to this problem is to carefully charac-

terize the materials - that is, to really identify them so that one can perform valid experiments. The general approach is to characterize the material before and after purification. All this leads to the rather disquieting conclusion that there is a great deal of uncertainty with respect to the nonaqueous data presently available. It is expected that the approach just described will better control the materials used and that the data generated can be reproduced and validly compared with other similarly obtained.

Some practical test results will now be discussed involving anodes, cathodes, and electrolytes. The electrolyte screening program produced significant numbers of nonaqueous solutions having conductivities greater than 10^{-3} ohm^{-1} centimeter^{-1}. Lithium, calcium, and magnesium as anodes were characterized in the best of these and several interesting systems capable of supporting substantial current densities evolved. Table II-4 shows some representative lithium anode systems. The dimethyl formamide system gassed badly. The $LiClO_4$-PC system has a high polarization at significant current densities and is thus shown to be a low rate system with a fairly low conductivity. It is, however, the one that has received the most attention. Of the stable systems shown, only $LiPF_6$-NDA has exhibited a 100 milliampere per square centimeter capability. It, as well as $LiClO_4$-MF, is receiving considerable attention for medium rate applications.

Table II-5 shows the cathodes presently of interest in the high energy density battery programs being supported by the government. As a result of these studies, there is confidence that workable primary systems are possible with what is now known. Now consider the Li-CuF_2 system using a $LiClO_4$-PC electrolyte. Figure II-27 shows a present laboratory cell design. It consists of a CuF_2 cathode between two lithium anodes. A separator on either side of the cathode prevents contact with the anodes. The cell is sealed in a plastic envelope and the electrolyte is inserted with a hypodermic syringe. It is then discharged through a constant resistance. Figure II-28 shows a typical discharge curve, cell potential being plotted against discharge time. This cell for an average current density of 0.5 milliampere per square centimeter produces a very constant voltage throughout the major portion of its discharge. The 3-volt potential is very desirable since reasonable battery output potentials can be obtained with a minimum number of cells in series. Figure II-29 compares Li-CuF_2 performance using a low rate PC electrolyte at 95° F with a medium rate MF electrolyte at 5° and 95° F. Energy densities in watt-hours per pound for the plastic envelope cell are plotted against discharge time. Note that values as high as 210 watt-hours per pound at 0.5 milliampere per square centimeter have been obtained at 95° F using PC as the solvent. If MF is the solvent, values as high as 170 watt-hours per pound at 5 to 10 milliamperes per square centimeter have been obtained at 5° F. At 95° F, however, the MF system is reduced to 60 to 90 watt-hours per pound, possibly due to increased reaction between the cell components. The solid line compares a conventional AgO-Zn cell's discharge characteristics. The most serious problem with these systems is the lack of shelf life. The cell using PC loses capacity by dissolution of CuF_2 into the electrolyte, diffusing away from the electrode and reacting with the lithium anode. Either a separator to prevent diffusion to the anode or an environment that prevents or drastically limits the solubility of CuF_2 is needed. Figure II-30 indicates that coulombic efficiency is reduced from 75 to 60 percent in 6 weeks when stored at 5° F. When stored at 95° F for 2 weeks, there is a change from 75 to about 20 percent. The Li-CuF_2 cell using a MF electrolyte suffers a more rapid degradation since lithium reacts readily with it. This system would require a reserve construction if built according to present technology.

One rather unique reserve construction is the dry tape battery shown in figure II-31. The anode, cathode, and an encapsulated electrolyte are contained in a plastic film or tape. On demand for power, the tape is passed between rollers, which crush the electrolyte capsules and thus allow the electrochemical reaction to proceed. Electric power is removed by current collectors on either side of the tape.

The microencapsulated tape, shown at the right in figure II-32 contains the anode, a separator, and the cathode with the microencapsulated electrolyte. Capsule diameters range from 500 to 1700 microns. Three practical problems hamper microencapsulation: first, electrolyte loading of only 42 to 70 percent by weight has been achieved; second, electrolyte utilization of only 50 percent further complicates the problem; and third, an electrolyte evaporation rate of 0.4 to 2 percent per day results in rather limited shelf life.

The macroencapsulated tape on the left reduces or eliminates these difficulties. In this design, larger packets of electrolyte are contained in the center of the tape which, when crushed, permeate the area between the electrodes. This design has proven more satisfactory.

Figure II-33 compares present dry tape performance with that of a conventional silver-zinc battery. The dry tape battery operates between 90 and 120 watt-hours per pound, almost independent of discharge rate. Note that the apparent efficiency drop off at high drain rates is at least partially due to applying the entire system's weight over a short discharge period. It is estimated that energy densities possible with present dry tape systems will approach 150 watt-hours per pound.

There is great interest in the development of secondary high energy density batteries since they have many potential applications. Several programs have been funded by NASA and other agencies in the past several years; the results have not been too encouraging from the practical standpoint, since a maximum of 15 to 30 cycles is the best reported performance. A Li-AgCl battery has demonstrated several hundred cycles, but this is not really a high energy density system being only about 10 percent better than silver-zinc.

The very slow rate of progress in the development of secondary batteries is due in large measure to the primitive understanding of the chemistry in these systems. Clearly it is impossible to make reasonable gains with such systems until some progress is made toward the identification of the species, the characterization of their equilibria, and some understanding of their transport properties. A wide variety of physical chemical measurements are needed to obtain this information. The process actually going on at the electrodes must be characterized, of course; but electrochemical studies by themselves will not give an adequate description for further progress. Several new programs are now underway where the emphasis is being placed on providing this insight. This effort should give sound direction to further development work in this important area.

FUEL CELLS

The high energy density reactants that have been discussed so far offer theoretical energy densities in the 500 to 800 watt-hours per pound range. There is a common reactant combination which theoretically can produce outputs over 1600 watt-hours per pound, and that combination is

hydrogen and oxygen. However, since these materials are low density fluids, it becomes necessary to use a different type of conversion device, namely, the fuel cell.

Figure II-34 illustrates that a fuel cell is essentially a continuous operating battery, with the invariance of the fuel cell the main distinguishing feature. In a battery, all reactant materials and the ensuing products of reaction are contained within the case, and thus the composition continually changes. In a fuel cell, on the other hand, fuel and oxidant are fed continuously to the cell and the reaction products continuously removed along with any heat produced by the reaction. Since the electrodes are unchanged, proper balance of the flow process leads to a constant invariant condition within the cell. As a result, the operating time is limited only by the supply of reactants. For long operating periods, the energy density can approach the theoretical value for the reactants since the weight of supporting hardware is constant.

The successes of fuel cells on five Gemini flights, coupled with the early qualification of the fuel cell for the Apollo spacecraft, have greatly increased confidence in their use. Operating times are being increased from the 2-week lifetime of Gemini and Apollo to 21 to 30 days for the biological satellites and 30 days or longer for the Air Force's manned orbiting laboratory. The availability of proven flight hardware and increasingly attractive life data are causing discussion of fuel cells for several thousand hours of operation and power levels of a few tens of kilowatts. The need for fuel cells for missions either currently defined or likely to appear in the next several years can be met by the several systems already qualified or nearing flight hardware status; therefore, the fuel cell work here emphasizes improvements in the basic hydrogen oxygen fuel cell rather than construction of systems competitive with those already in existence. Efficiencies of the hydrogen-oxygen cells are high so that no large improvements in energy density are possible. As a result, the work done here has emphasized stable operation for long periods of time at the highest possible efficiency.

One of the critical areas demanding attention is the development of electrode materials capable of high power output and long life. The initial effort was directed toward improving the energy conversion capability and extending the operating environment of the lightweight-deposited catalyst nickel screen electrode.

New catalyst materials, including platinum blacks and platinum-rhodium mixtures were prepared and evaluated. A variety of nickel support screens was tested singly and in sandwich configurations. Levels of Teflon waterproofing between 8 and 50 percent were investigated.

This research activity resulted in an electrode, manufactured by the American Cyanamid Company and designated the AB-40, which uses a 40 milligram per square centimeter deposited platinum black catalyst supported on a 40-mesh nickel screen with 25 percent Teflon waterproofing. The nickel screen is gold plated to deter oxidation of the nickel when the electrode was used as a cathode in a hydrogen-oxygen fuel cell.

In the evaluation of these electrodes, single test cells were constructed using the AB-40 material for both anode and cathode. A matrix-separator, containing the electrolyte, was sandwiched between them.

Figure II-35 shows the performance obtained in single cell testing using the AB-40 electrode with a Johns Manville Quintera asbestos matrix containing a 50-percent KOH electrolyte concentration. The lower curve was run at a temperature of 160° F and atmospheric reactant pressure. The center curve demonstrates that increasing the operating temperature to 212° F results in a

10-percent improvement in cell output. An additional 10 percent is realized by increasing the reactant pressure to 45 pounds gage. The decrease in the rate of potential dropoff in the two top curves results from a decrease in the electrolyte concentration polarization due to increased ion mobility at higher temperature and a lower gas side polarization at higher reactant pressures.

The Quintera matrices of these cells have also demonstrated reliable life at current drains up to 300 amperes per square foot, as shown by figure II-36 in which cell potential against operating life in hours is plotted for several current densities.

The cell represented in the top curve was initially at a load of 100 amperes per square foot for 1450 hours after which the load was increased to 200 amperes per square foot. This cell is still operating after more than 4000 hours at a potential of 0.83 volt. For reference, it should be noted that 4000 hours is almost 6 months.

The cell operating at 200 amperes per square foot has run more than 1800 hours with a potential loss of only 2 percent, or 18 millivolts. Though the potential of the cell operating at 300 amperes per square foot is dropping off more rapidly, it has only decreased 5 percent, or 40 millivolts, in 1700 hours. This cell does, however, demonstrate that control problems increase at higher current levels.

In one of the earlier slides, the improved performance at higher temperatures was noted. It was found, however, that at temperatures above 212° F with electrolyte concentrations of 50 percent KOH, the asbestos matrix materials tended to dissolve, leading to cell failure.

In a search for higher temperature materials, the American Cyanamid Company has developed a ceria-Teflon material which resists electrolyte attack up to 300° F.

The performance of single cells using the ceria-Teflon matrix is shown in figure II-37. Here again, the improvement at higher temperatures and reactant pressure is evident. The dashed line is a comparison curve for a Quintera matrix run under the same conditions as the lower ceria-Teflon test. It is apparent that at temperatures of 212° F and below, the Quintera matrix offers superior performance and would be selected for applications in that range.

Life test with the ceria-Teflon matrix has not been as extensive as with the Quintera matrix since this is a development matrix and has only recently been characterized. Figure II-38 shows that 1000 hours of life has been demonstrated at temperatures of 260° F and 60-percent KOH concentration at current loads of 100 and 200 amperes per square foot. Two recently started tests at 100 and 200 amperes per square foot with reactant pressures of 45 psig are progressing quite satisfactorily after 500 hours. The increase in cell potential with increased reactant pressure at 200 amperes per square foot approaches 70 millivolts for a resultant 14-percent power gain.

Results to date with the American Cyanamid electrode have demonstrated that moderate and high current levels can be attained at reasonable cell potentials. Sufficient life test experience at moderate current density indicates that the electrode and matrix materials will hold up for 2000 to 4000 hours. The electrode-matrix development effort at Cyanamid is continuing and preparations are being made to evaluate these materials in a fuel cell module and in a complete system here at Lewis.

One unusual application for the hydrogen-oxygen fuel cell is as a secondary battery. Such a battery consists of a number of fuel cells, connected in series, which operate in the normal fashion during discharge and as electrolysis cells during charge. The gases generated on charging are stored in tanks which are an integral part of the battery. Figure II-39 shows a typical test vehicle.

There is a six-cell fuel cell stack in the center with the hydrogen storage tank on the left and the oxygen tank on the right. A pressure-balancing bellows, not shown here, prevents any appreciable pressure differential from being established across the cell.

This device offers a number of operational advantages. Cell reversal is impossible, and high overcharge rates can be sustained, limited only by the unit's ability to dissipate heat. This device has also operated satisfactorily after thermal sterilization. The most significant advantage, however, is that this is the only secondary battery in existence which gives a positive, accurate, state-of-charge indication. Figure II-40 shows a typical charge-discharge cycle. Note that the tank pressure increases linearly with charge and decreases linearly during discharge as a function of the current passed. By monitoring tank pressure, the exact state-of-charge can be determined.

Figure II-41 shows a 500-watt, 600 watt-hour battery that has been tested. The 34-cell stack is to the right of the center flange, and the pressure-balancing bellows to the left. The body of the unit is $8\frac{1}{2}$ inches in diameter and 37 inches long. It weighs 39 pounds as shown, but it is estimated that as a flight unit it would weigh 30 pounds and thus could deliver 10 watt-hours per pound in low-altitude orbit and 20 watt-hours per pound in a 24-hour orbit. The overall efficiency is 58 percent, which compares favorably with conventional secondary batteries. Power outputs over 1300 watts have been delivered for short times.

Like all experimental devices, this one has problems. For one, its volume is approximately three times that of an equivalent battery. Self-discharge occurs due to the high tank pressures, and charged-stand times beyond a few weeks appear impractical.

The most serious problem is life. The best results to date have been 300 cycle (500 hr) on multicell units and 725 cycles (6 weeks) on single cells. The present effort is concentrated on solving these life problems in order to enhance the usefulness of this battery.

The discussion on hydrogen-oxygen fuel cells thus far has studiously avoided mentioning a rather weighty problem - how the hydrogen and oxygen are to be stored. The problems of storing hydrogen and oxygen lead one to consider those materials which are easily stored on a spacecraft - that is, storable rocket propellants. An additional incentive for their use is the fact that they might just be along for the ride anyway and what is left over in the fuel cells can be used.

The first stage in the development of fuel cells using storable rocket propellants was to determine which, if any, were feasible electrochemically. Of the fuels only N_2H_4, which was electroactive in acidic and basic electrolyte, showed feasibility. The UDMH was unreactive. Aerozine 50 is a 1:1 mixture of N_2H_4 and UDMH. As to be expected, only the N_2H_4 portion of it was active. Of the oxidizers, only N_2O_4 and HNO_3 showed feasibility. The H_2O_2 spontaneously decomposed at a too rapid rate. The potentials generally observed for hydrazine and hydrogen are similar. This is not unexpected since it is well known that hydrazine with its positive free energy of formation decomposes readily upon a suitable catalytic surface. Furthermore, the same general loss of potential occurs in acid electrolyte with both hydrazine and hydrogen. It is quite probable, therefore, that hydrazine functions as hydrogen when anodically oxidized. The choice of catalysts is quite critical since one that is too active causes excessive spontaneous decomposition and one that is not active enough reduces the electrochemical utilization. Since a very active catalyst decomposes N_2H_4 to hydrogen, the oxidizer can also be decomposed to oxygen and then used in any hydrogen-oxygen fuel cell. Thus, the present program has emphasized decomposing

N_2H_4 and Aerozine 50 to obtain hydrogen, and N_2O_4 to obtain oxygen. The Aerozine 50 reactor is shown schematically in figure II-42.

Aerozine 50 and water contact first a zinc catalyst, then a nickel oxide catalyst, and finally an iron oxide catalyst. The stream then passes through a palladium diffuser to produce ultrapure hydrogen. The reactor output composition is shown at the bottom of figure II-42.

Figure II-43 shows how the efficiency varies with time. Percent of hydrogen obtained is plotted against hours of continuous operation. Initially the process is about 99 percent efficient, but quickly levels off to slightly better than 95 percent for 1000 hours of continuous operation. Figure II-44 shows a N_2O_4 reactor. It uses 2 percent platinum on Al_2O_3. This system starts out at a rather high value but after 80 hours has fallen to about 80 percent. It is apparently quite stable at this value up to 1000 hours of continuous operation. The oxygen inefficiency is caused by a deactivation of the catalyst to a constant level of performance and allows N_2O_4 to be admitted to the fuel cell cathode. This is undesirable, especially for an alkaline electrolyte system. Limited studies with zeolites indicate that they can effectively remove the N_2O_4. Studies are now underway to demonstrate their useful life and efficiency.

CONCLUSIONS

A variety of programs has been presented herein. It might be well to consider what the future holds for some of the resulting systems.

In assessing the signficance of the different types of battery work described, the natural tendency is to refer to the baseline values of 30 to 90 watt-hours per pound for primary cells, and perhaps 2 watt-hours per pound for long-life secondary cells, and to conclude that the most important programs are those which promise to raise these values the greatest amount. One would then assume that the nonaqueous work is of greatest significance, and in fact, a large part of our battery technology program is oriented in that direction. However, much research is needed and complete development of such batteries will take a long time, if it comes about at all. As a result, it may turn out that incremental improvements in existing batteries, which will be used over and over again, will be more important in the long run. Certainly the development of a long-cycle life silver-zinc cell will be a significant increase in the state of the art for secondary batteries.

In fuel cells, it is unlikely that any system will unseat the hydrogen-oxygen system from its prominent position, although others may be developed to meet special needs. Therefore, any technology work on this system is a good long-term investment.

Beyond that, one cannot guess which of the programs described herein will be of greatest value. It can only be said that several of these efforts will find eventual use in flight programs.

REFERENCES

1. Conway, B. E.; and Bourgault, P. L.: Electrochemistry of the Nickel Oxide Electrode. Part III. Anodic Polarization and Self-Discharge Behavior. Can. J. Chem., vol. 40, no. 8, Aug. 1962, pp. 1690-1707.

2. Pitman, A. L.; and Work, G. W.: Alkaline Storage Batteries - An Investigation of Nickel Oxide Positive Plate Characteristics. Rep. No. 5031 (DDC No. AD-149784), Naval Research Lab., Dec. 2, 1957.

3. Ritterman, P.; Lerner, S.; and Seiger, H.: Investigation of Battery Active Nickel Oxides. Gulton Industries, Inc. (NASA CR-72018), June 12, 1966.

4. Salkind, Alvin J.; and Bruins, Paul F.: Nickel-Cadmium Cells. I. Thermodynamics and X-Ray Studies. Electrochem. Soc. J., vol. 109, no. 5, May 1962, pp. 356-360.

5. Labat, Jean: Nickel Hydroxides. Ann. Chim., vol. 9, no. 7-8, 1964, pp. 399-427.

6. Ritterman, P.; Lerner, S.; and Seiger, H.: Investigation of Battery Active Nickel Oxides. Gulton Industries, Inc. (NASA CR-54957), Mar. 12, 1966.

7. Kober, Frederick P.: Analysis of the Charge-Discharge Characteristics of Nickel-Oxide Electrodes by Infrared Spectroscopy. Electrochem. Soc. J., vol. 112, no. 11, Nov. 1965, pp. 1064-1067.

8. Ritterman, P.; Lerner, S.; Seiger, H. N.; and Vaughan, P.: The Structure of the Battery Active Materials Existing on the Sintered Nickel Oxide Electrode at Various Stages of Charge. Paper to be presented at the Philadelphia Meeting of the Electrochemical Society, Philadelphia, Pennsylvania, Oct. 9-14, 1966.

9. Harris, William S.: Electrochemical Studies in Cyclic Esters. Rep. No. UCRL-8381, University of California, Radiation Lab., July 17, 1958.

10. Harned, Herbert S.; and Owen, Benton B.: Physical Chemistry of Electrolytic Solutions. 2nd ed. Reinhold Publ. Corp., 1950, p. 192.

11. Elliott, W. E.; Hsu, S. L.; and Towle, W. L.: The Development of High Energy Density Primary Batteries, 200 WATT Hours per Pound of Total Battery Weight Minimum. Final Rep. (NASA CR-54153), Globe-Union, Inc., Jan. 1965.

TABLE II-1. - THEORETICAL ENERGY DENSITIES OF HIGH ENERGY COUPLES

Anode-cathode	Theoretical potential, V	Theoretical reactant performance, (W-hr)/lb
Li-$CuCl_2$	3.07	503
Li-CuF_2	3.55	749
Mg-ACL	2.92	785
Zn-AgO	1.86	205

TABLE II-2. - MAXIMUM CONDUCTIVITIES OF SELECTED ELECTROLYTES

Solvent	Solute	Specific conductance, $ohm^{-1}\text{-}cm^{-1}$
Water	KOH	55.0×10^{-2}
Methyl formate	$LiClO_4$	2.6
Propylene carbonate	$LiClO_4$	.5

TABLE II-3. - VOLTAGE LOSS DUE TO ELECTROLYTE RESISTANCE

Electrolyte	Voltage loss at current density of 10 mA/cm^2, V
KOH-H_2O	0.0018
$LiClO_4$-MF	.0385
$LiClO_4$-PC	.2000

TABLE II-4. - LITHIUM ANODE PERFORMANCE

Electrolyte		Polarization, V		Compatibility
Solvent	Solute	10 mA/cm^2	100 mA/cm^2	
DMF	$(n\text{-}C_4H_9)_4NPF_6$	0.4	1.0	Gases vigorously
NDA	$LiPF_6$	.2	1.6	Stable
PC	$LiClO_4$	.6	>3.0	Stable

TABLE II-5. - CATHODE SYSTEMS

Cathode	Electrolyte	Application
CuF_2	$LiClO_4$-PC	[a]Low rate
$CuCl_2$	$LiAlCl_4$-PC	[b]Medium rate
CuF_2	$LiClO_4$-MF	[b]Medium rate
AgO	$LiPF_6$-NDA	[b]Medium rate

[a]Current densities to 1 mA/cm^2.
[b]Current densities from 1 to 10 mA/cm^2.

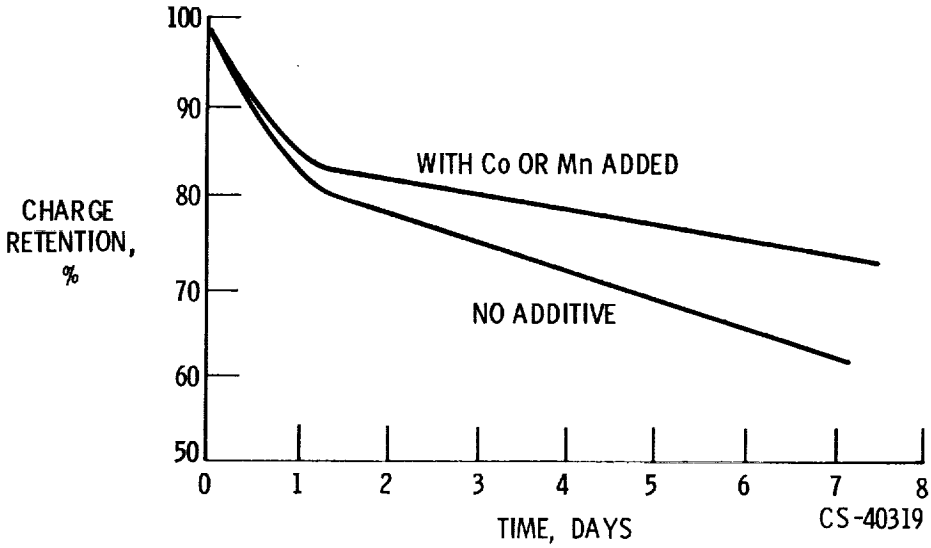

Figure II-1. - Stability of charged nickel oxide electrodes at 150° F.

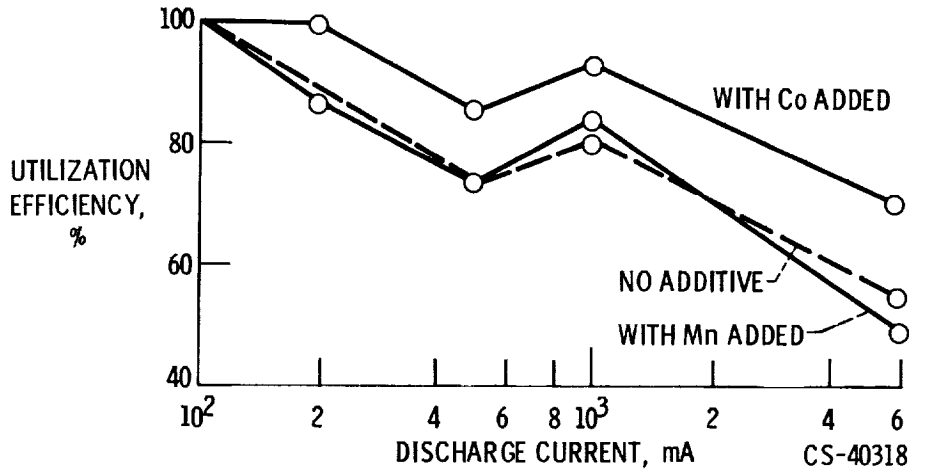

Figure II-2. - Utilization efficiency of nickel oxide electrodes as function of discharge current.

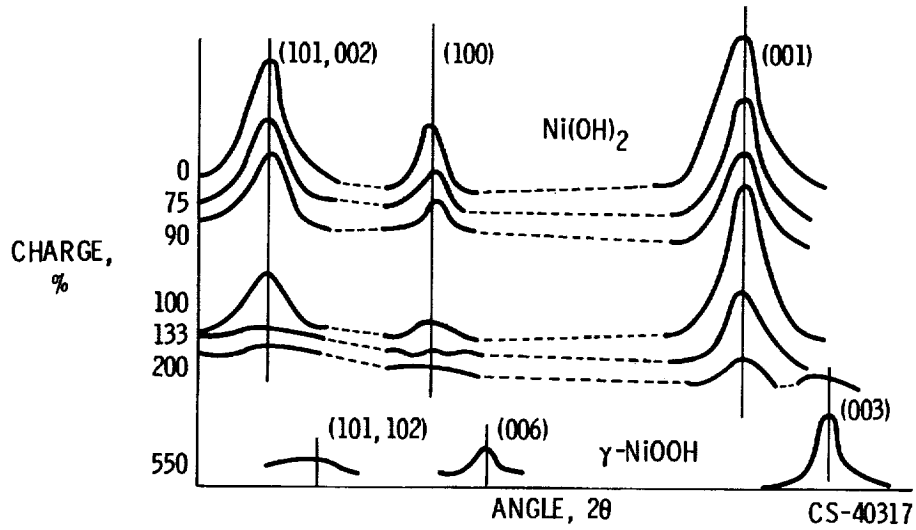

Figure II-3. - Nickel oxide electrode, X-ray diffraction.

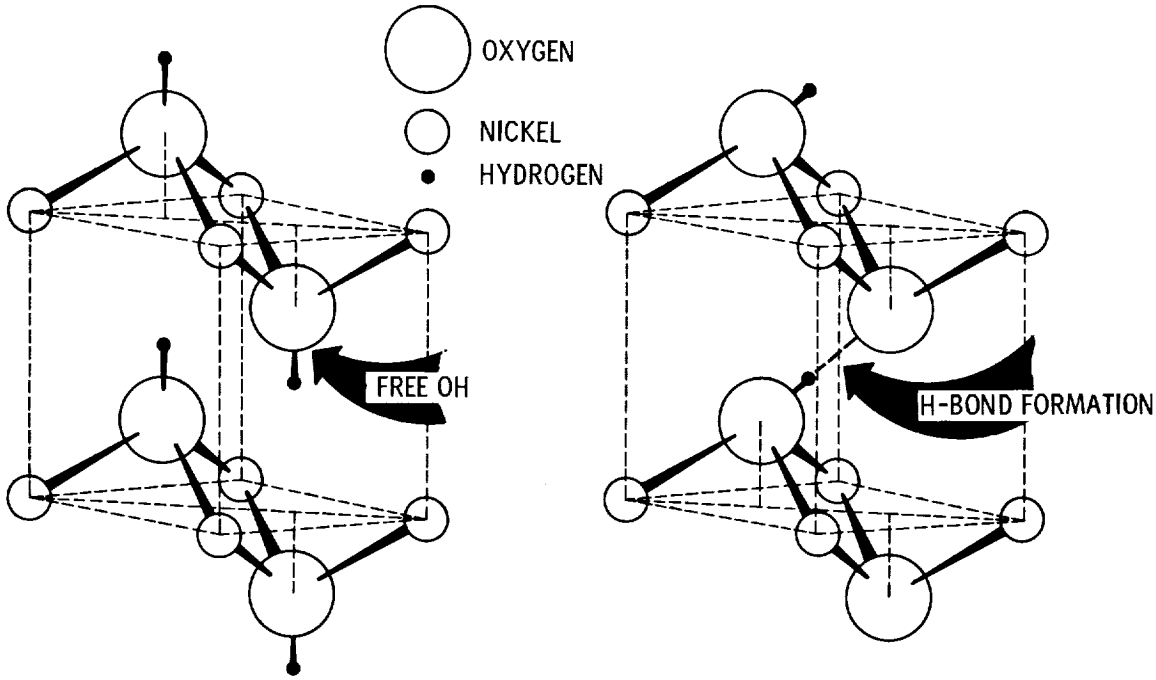

(a) Discharge state, nickel hydroxide.

(d) Up to 90 percent charged.

Figure II-4. - Structure of material in nickel oxide electrode.

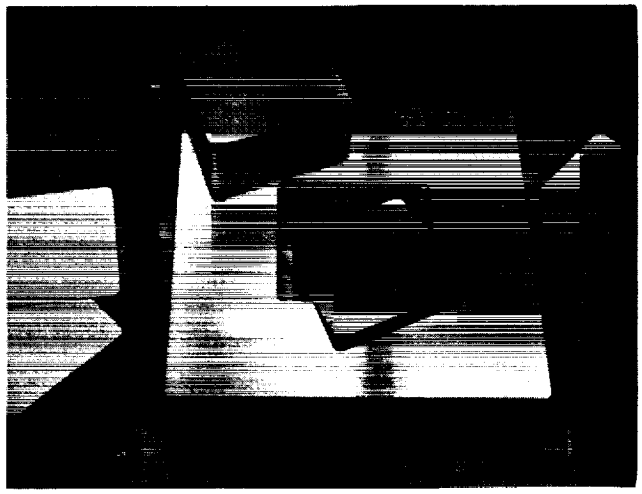

CS-40390

Figure II-5. - Inorganic cell separator.

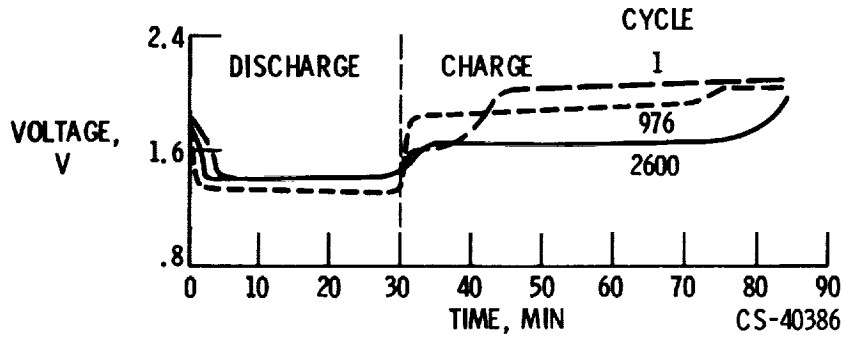

Figure II-6. - Experimental silver-zinc secondary cell. Charge-discharge cycle test at 77° F; depth of discharge based on 16-hour discharge, 17 percent.

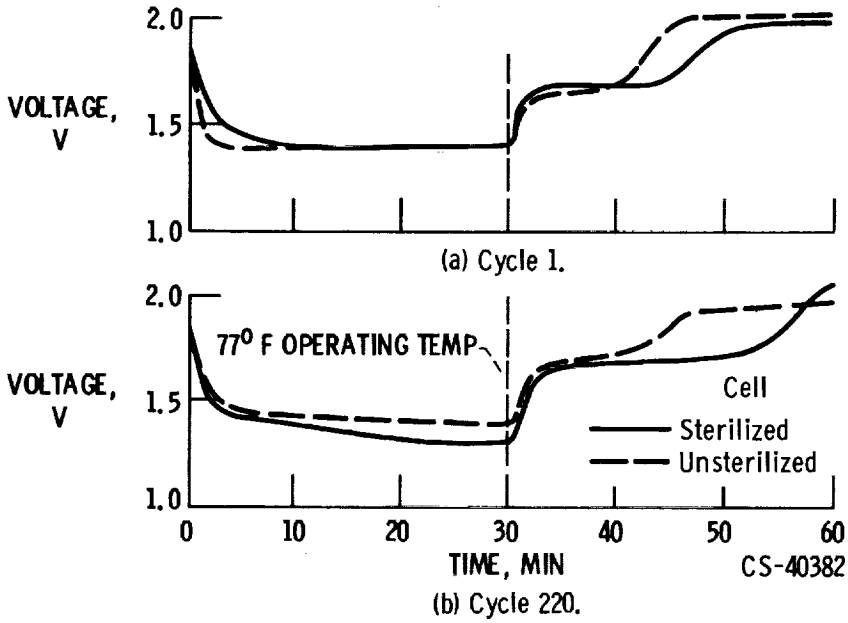

Figure II-7. - Experimental silver-zinc cell after thermal sterilization for 108 hours at 293° F.

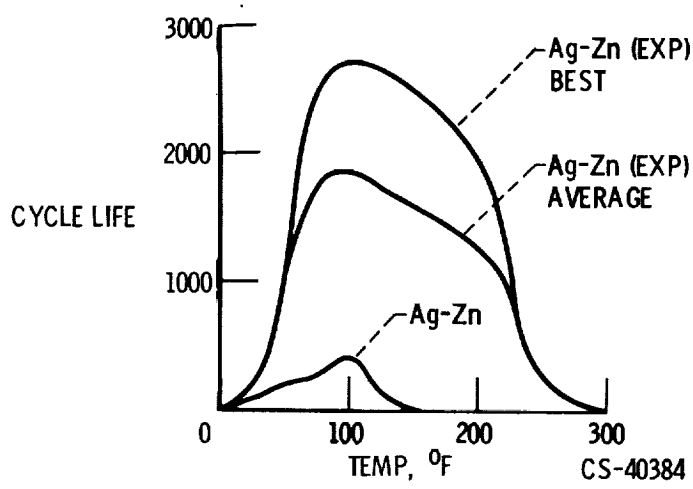

Figure II-8. - Comparison of cycle life of silver-zinc batteries. Depth of discharge, 25 percent.

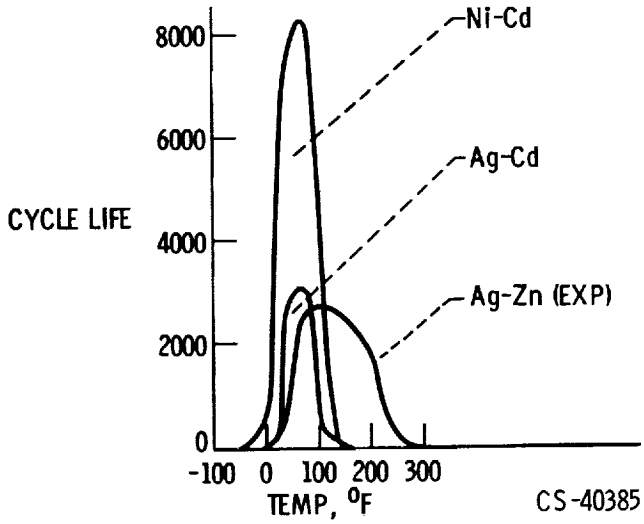

Figure II-9. - Comparison of cycle life of secondary batteries against temperature. Depth of discharge, 25 percent.

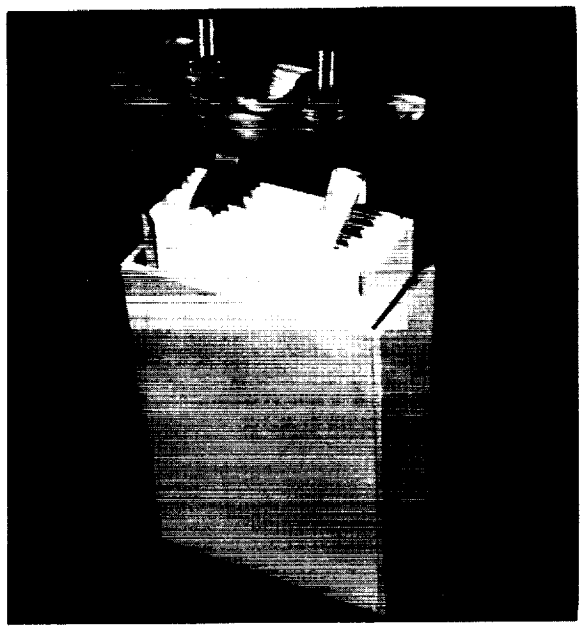

CS-40389

Figure II-10. - Silver-zinc cell assembly.

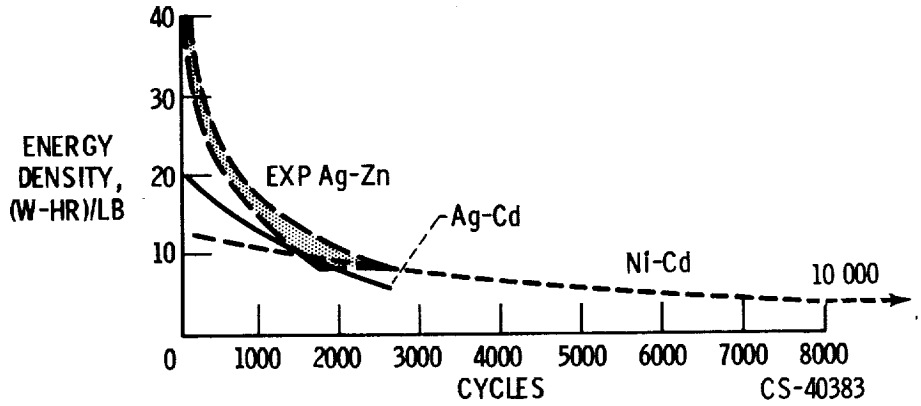

Figure II-11. - Comparison of energy density with cycle life.

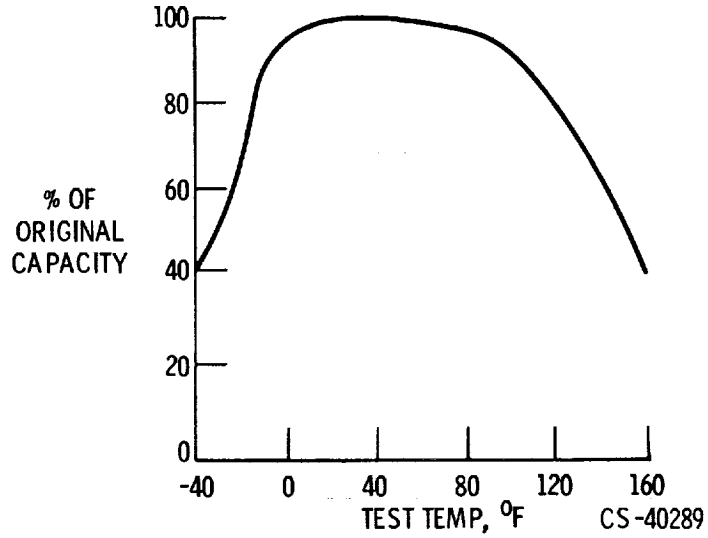

Figure II-12. - Loss of capacity of silver-zinc battery as function of temperature (after 2-wk wet stand at test temperature, fresh battery at 80° F equals 100 percent).

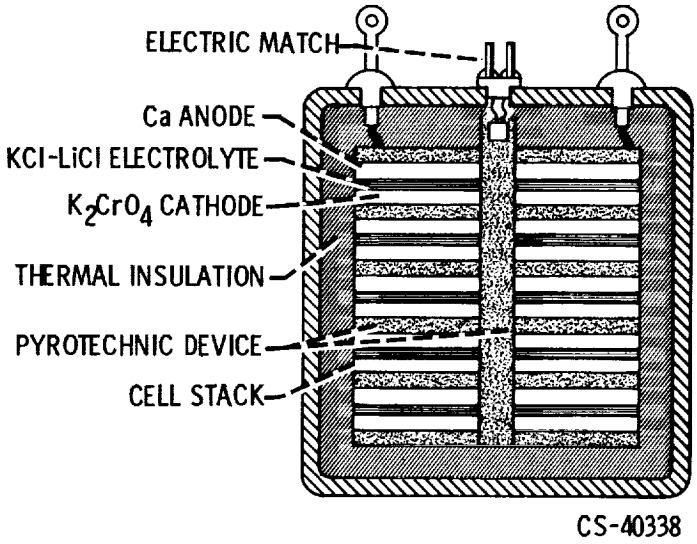

Figure II-13. - State of the art of high-temperature battery. Typical performance: service life, 5 minutes; operating temperature, 800° F.

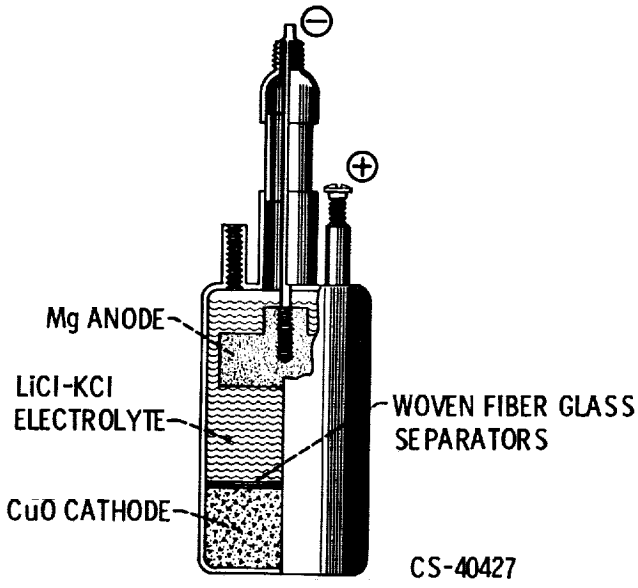

Figure II-14. - NASA experimental high-temperature cell.

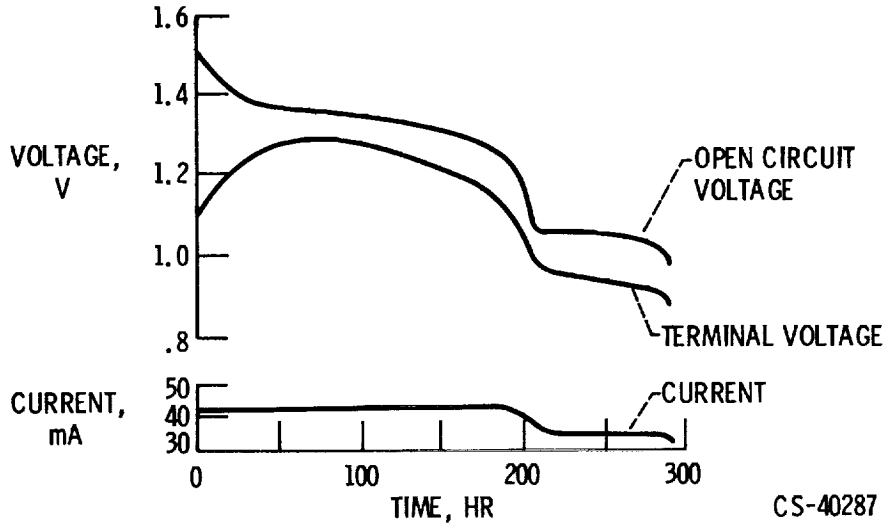

Figure II-15. - Performance of Mg-LiCl - KCl-CuO cell at 830° F.

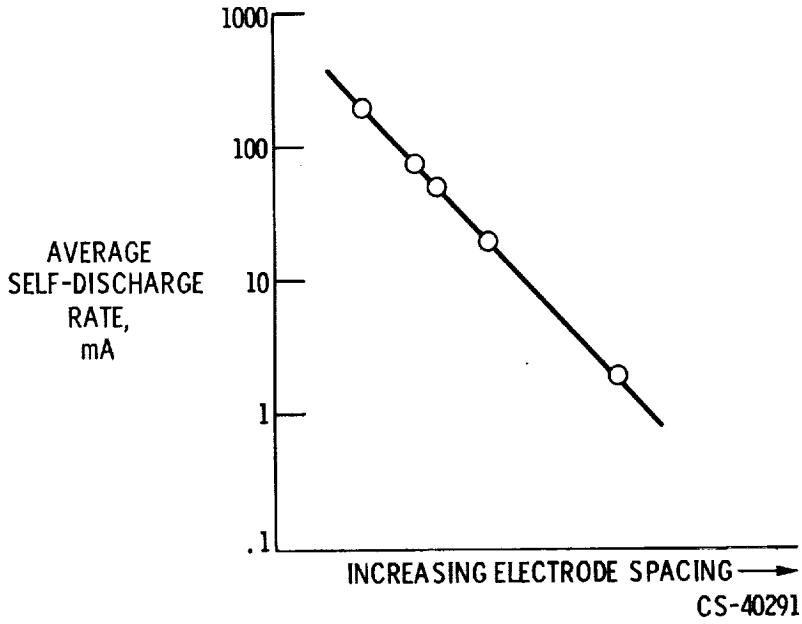

Figure II-16. - Effect of cell configuration on self-discharge rate.

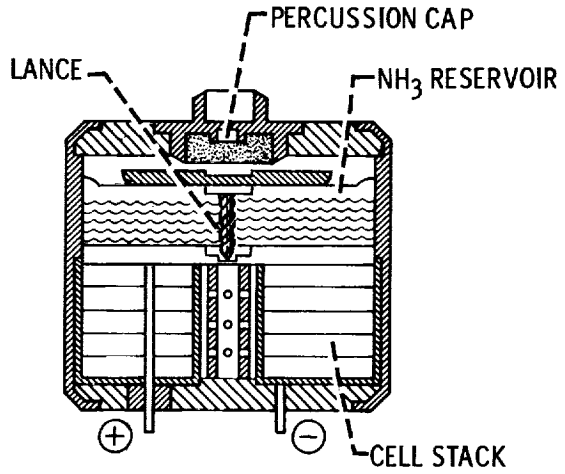

Figure II-17. - State of the art of low-temperature battery. Typical performance: service life, 36 hours; operating range, -65^0 to 160^0 F.

CS-40337

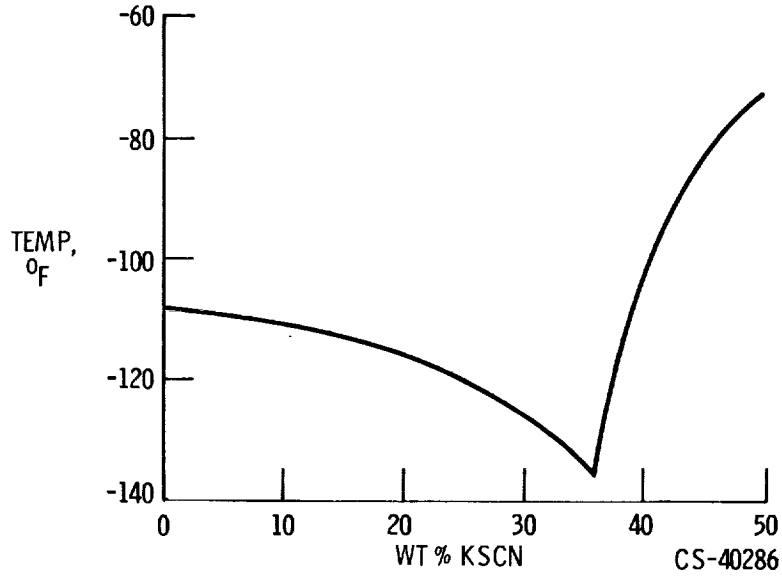

Figure II-18. - Freezing point diagram of NH_3 - KSCN.

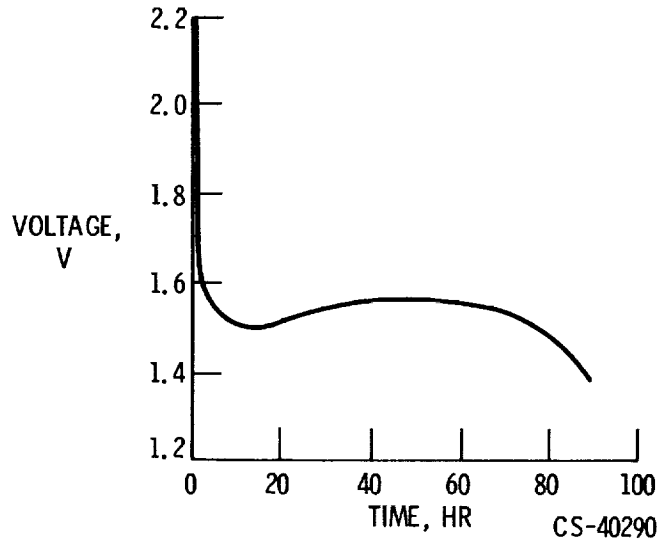

Figure II-19. - Performance of $Mg-NH_3$ - KSCN-S cell at -130^0 F.

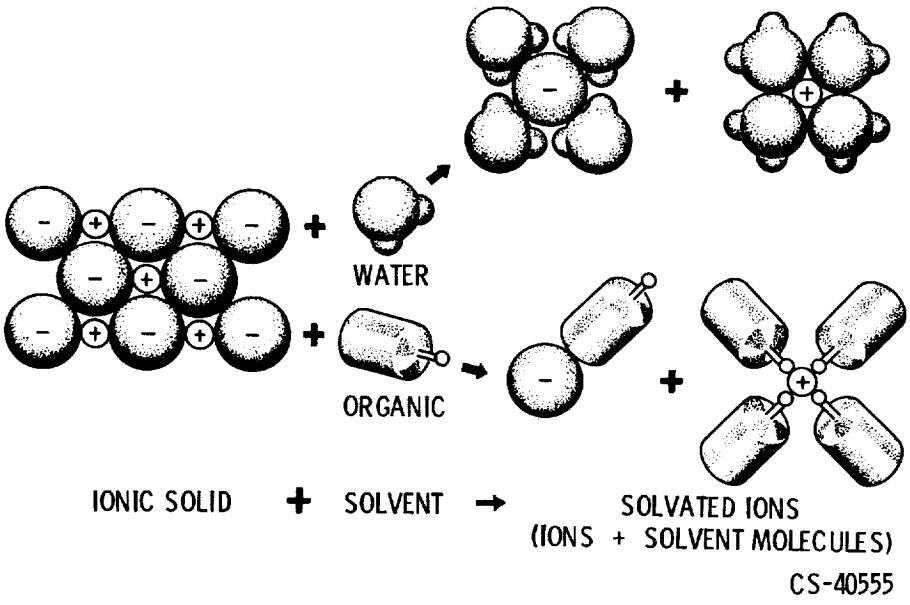

Figure II-20. - Dissolving an ionic solid.

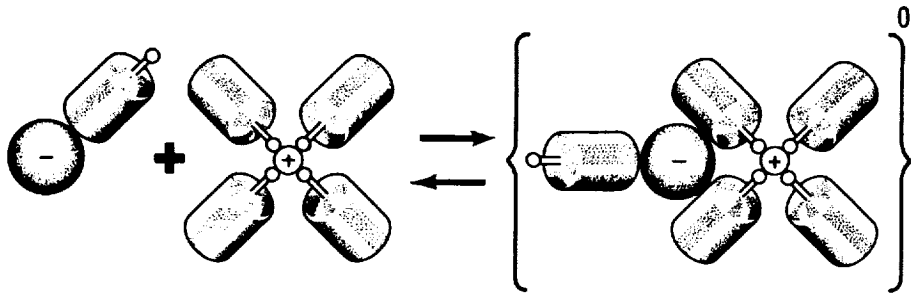

Figure II-21. - Ion pair equilibrium.

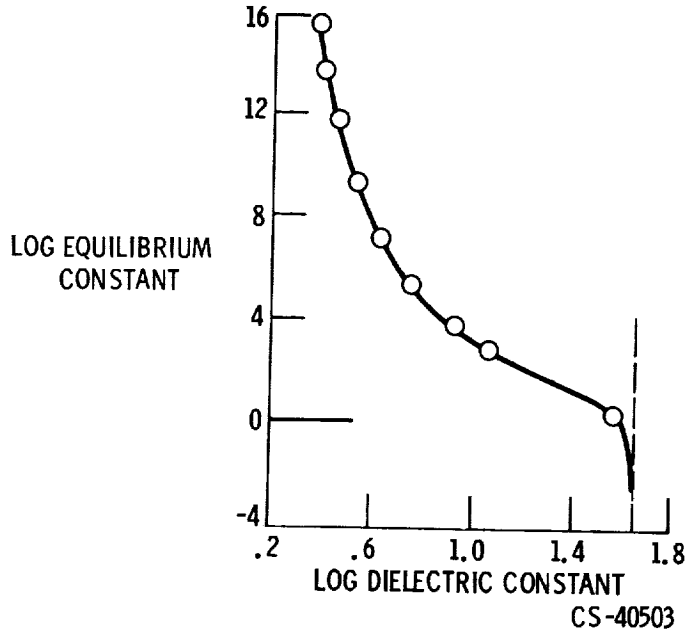

Figure II-22. - Ion pair formation as function of dielectric constant. $C^+ + A^- \rightleftarrows [C^+A^-]^0$ (after Fuoss and Kraus).

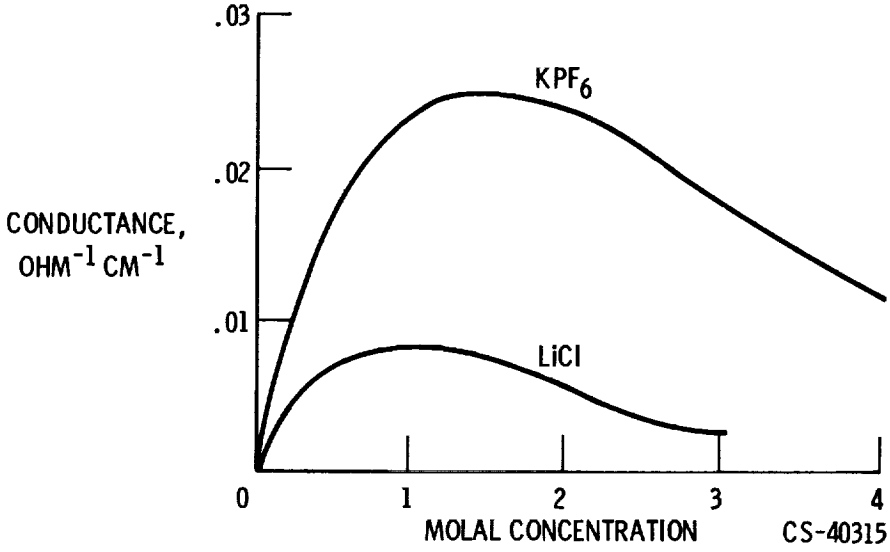

Figure II-23. - Conductance of solutions of salts in dimethyl formamide.

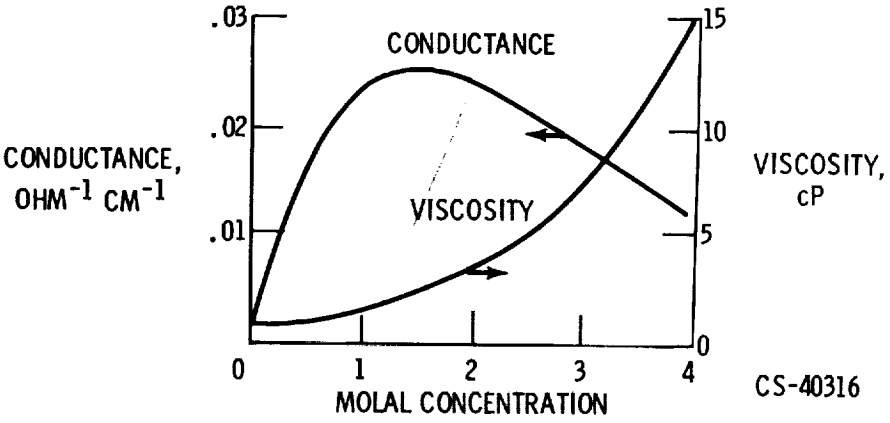

Figure II-24. - Conductance and viscosity of KPF_6 in dimethyl formamide.

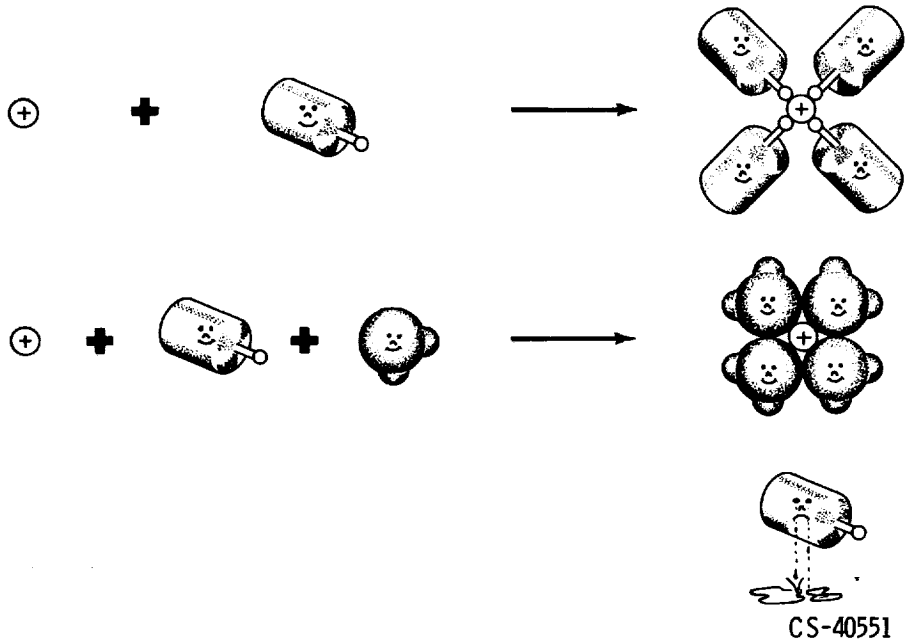

CS-40551

Figure II-25. - Preferential solvation.

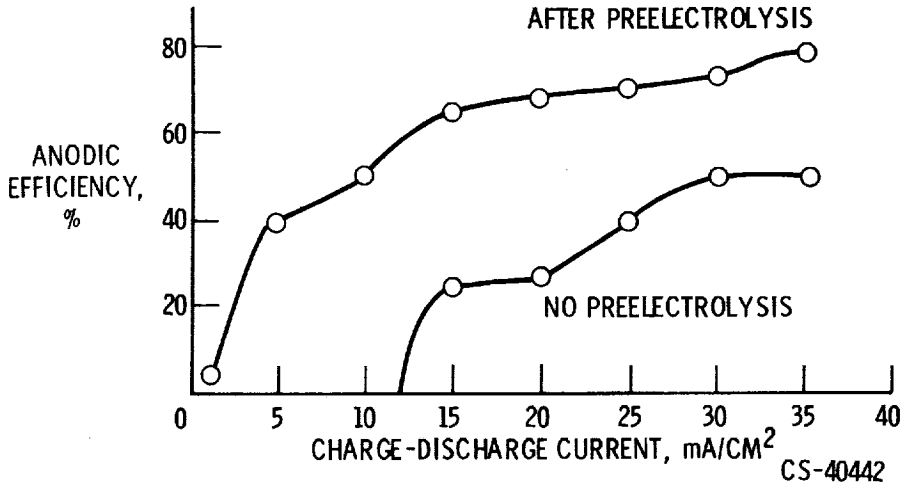

CS-40442

Figure II-26. - Effect of preelectrolysis on lithium anodic efficiencies. Prelectrolyzed and nonpreelectrolyzed electrolyte composed of propylene carbonate, 0.4M $AlCl_3$, and 0.35M LiCl.

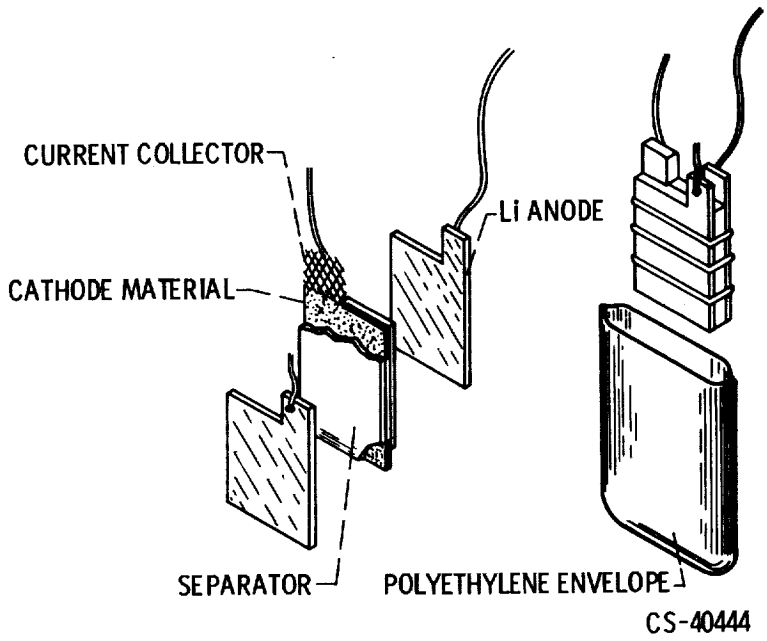

Figure II-27. - High energy density laboratory test cell.

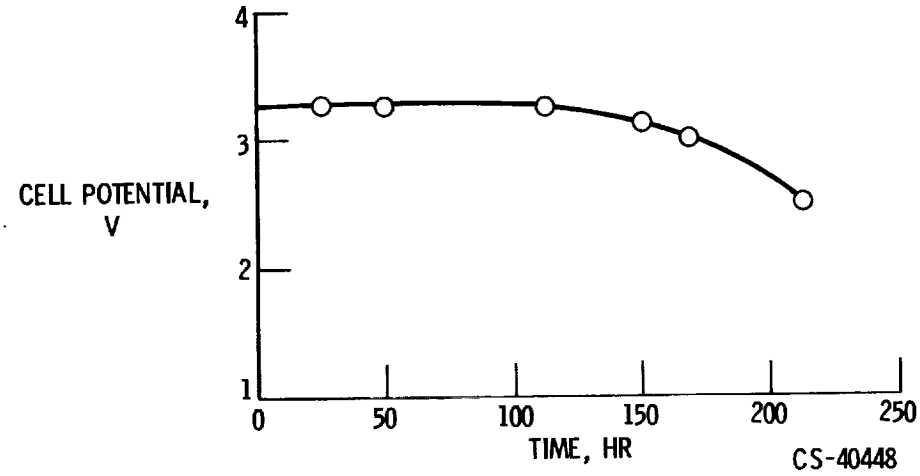

Figure II-28. - Discharge characteristics of Li-CuF_2 cell.

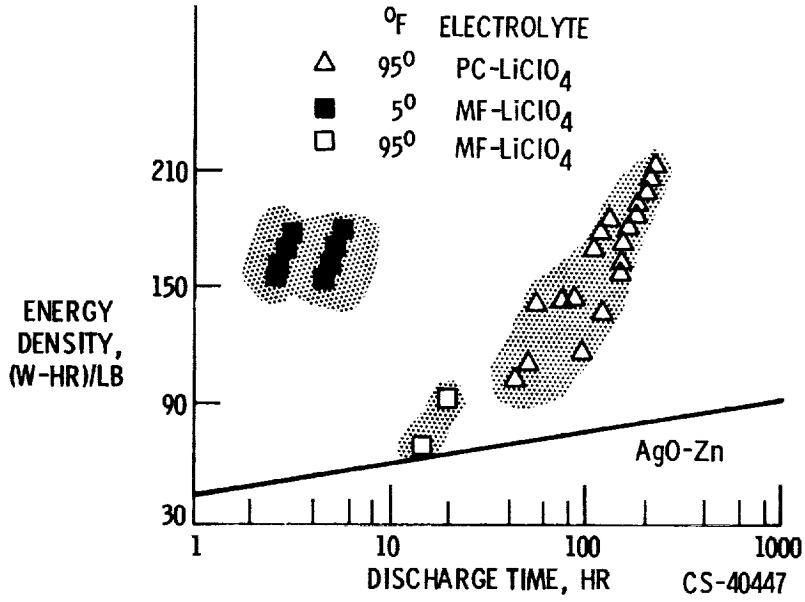

Figure II-29. - Cell performance of Li-CuF_2.

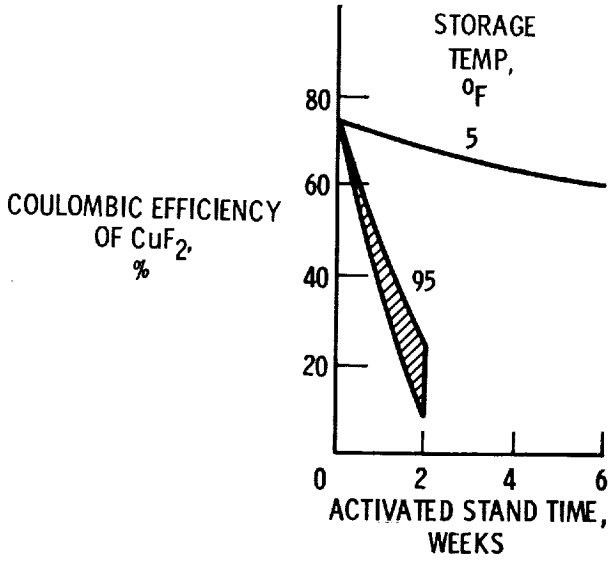

Figure II-30. - Shelf life of Li-CuF_2 cells stored at 5^0 and 95^0 F. Electrolyte, $LiClO_4$ - propylene carbonate.

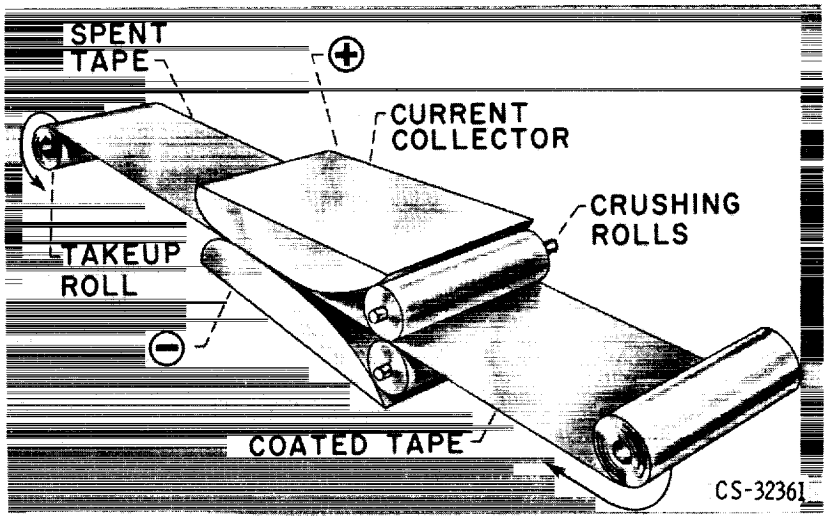

Figure II-31. - Dry tape battery concept.

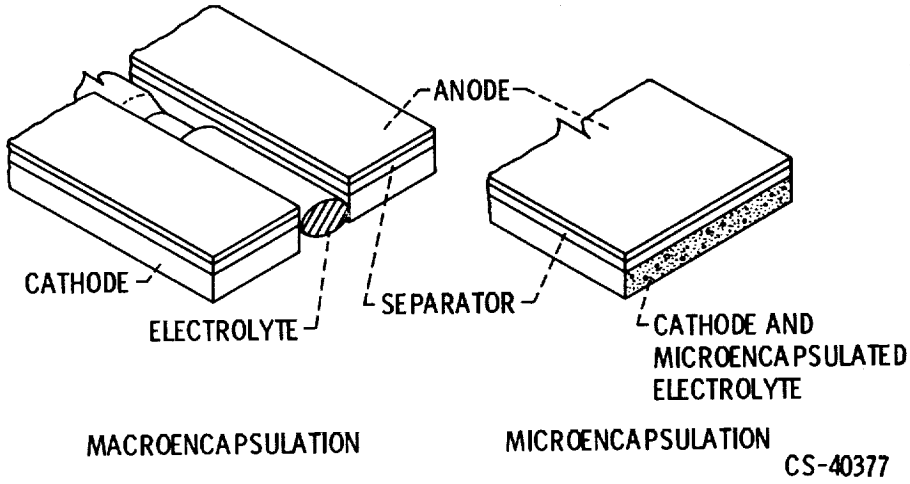

Figure II-32. - Dry tape concepts.

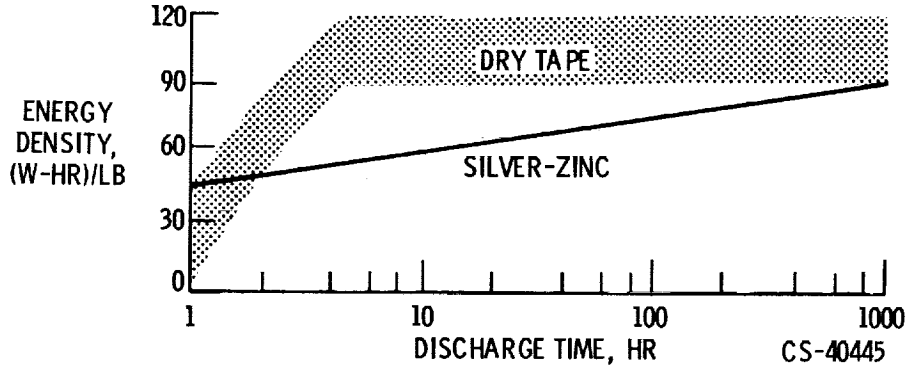

Figure II-33. - Aqueous dry tape performance.

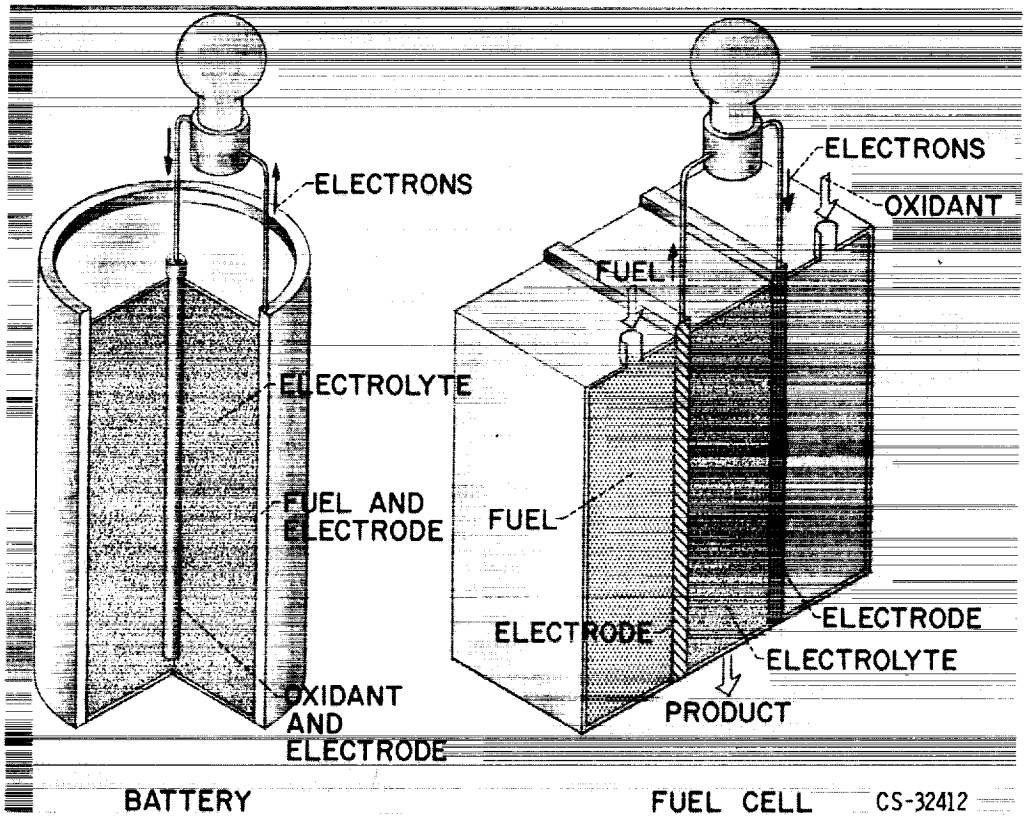

Figure II-34. - Comparison of battery and fuel cell.

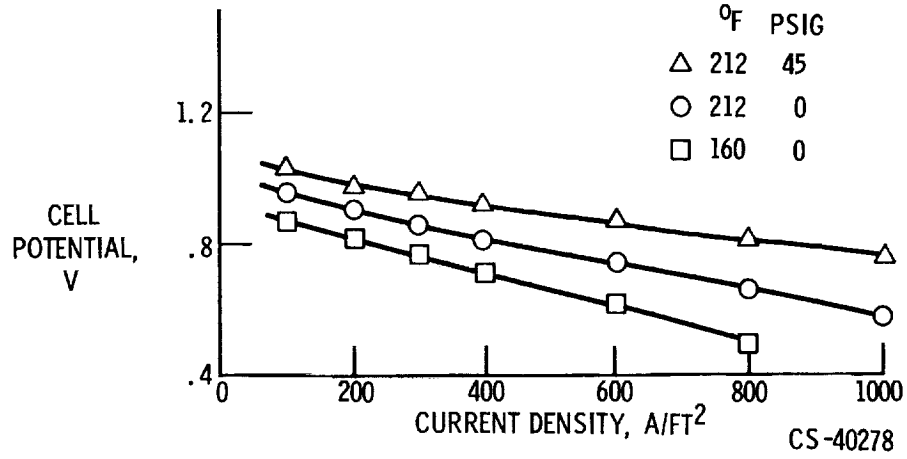

Figure II-35. - Single cell performance for cyanamid AB-40 electrode with Quintera matrix and 50 percent KOH.

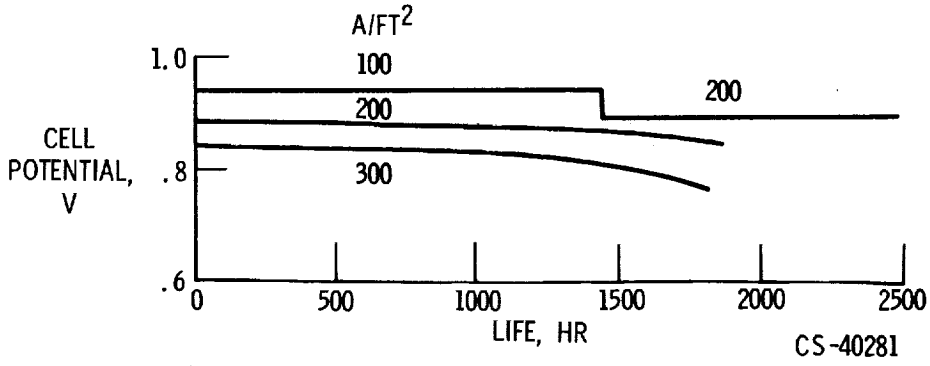

Figure II-36. - Life test for cyanamid AB-40 electrodes with Quintera matrix. Operating conditions: 212° F, 50 percent KOH, 0 psig.

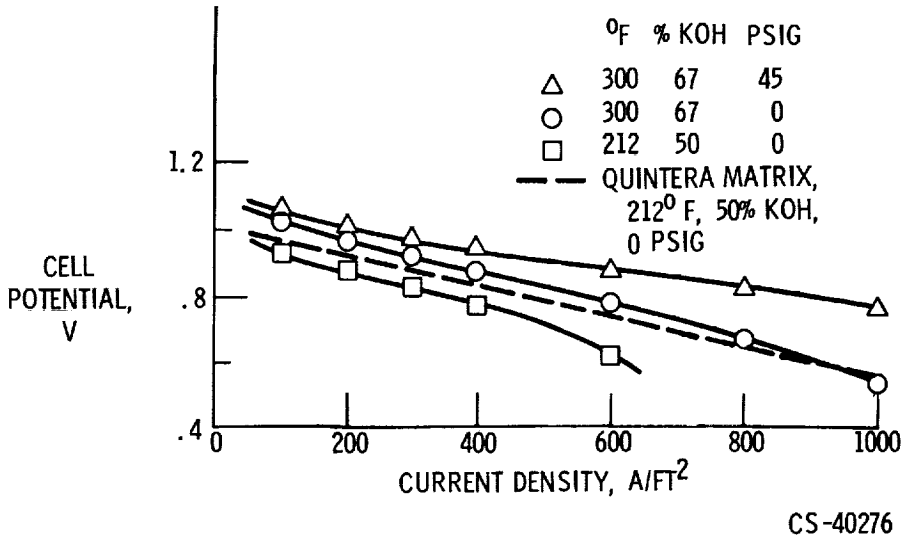

Figure II-37. - Single cell performance of cyanamid AB-40 electrode with ceria-Teflon matrix.

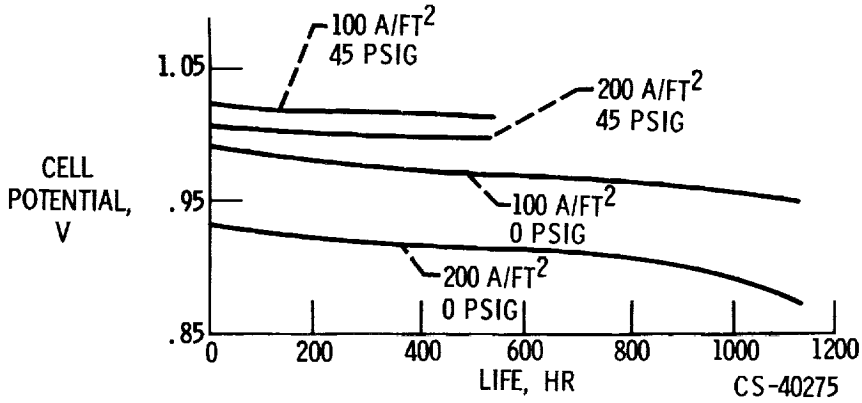

Figure II-38. - Life test for cyanamid AB-40 electrode with ceria-Teflon matrix. Operating conditions: 260° F; 60 percent KOH.

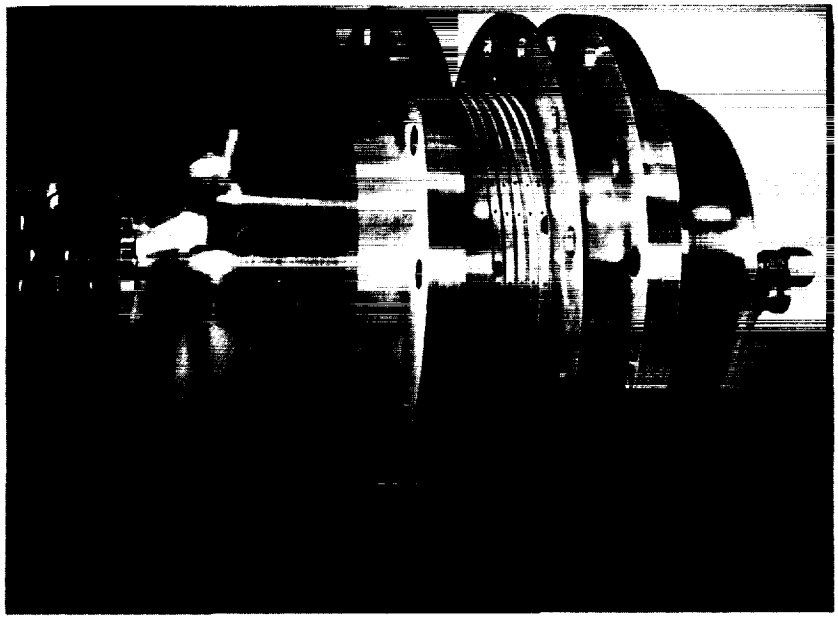

CS-40392

Figure II-39. - Six-cell regenerative hydrogen-oxygen unit.

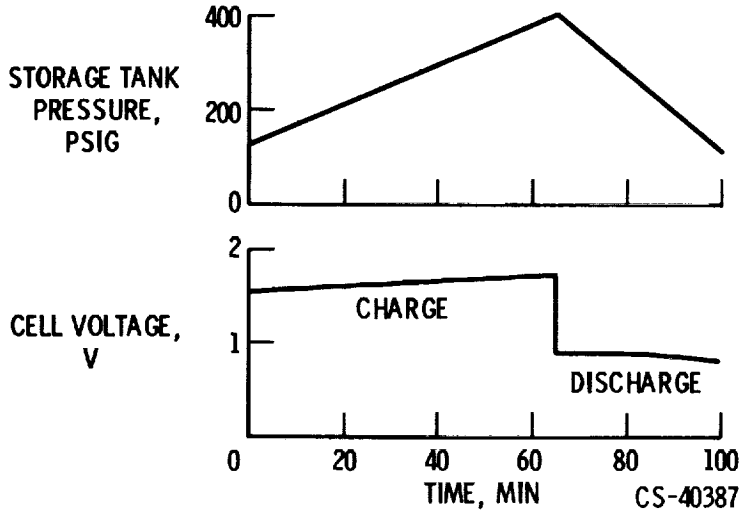

Figure II-40. - Performance of regenerative hydrogen-oxygen fuel cell.

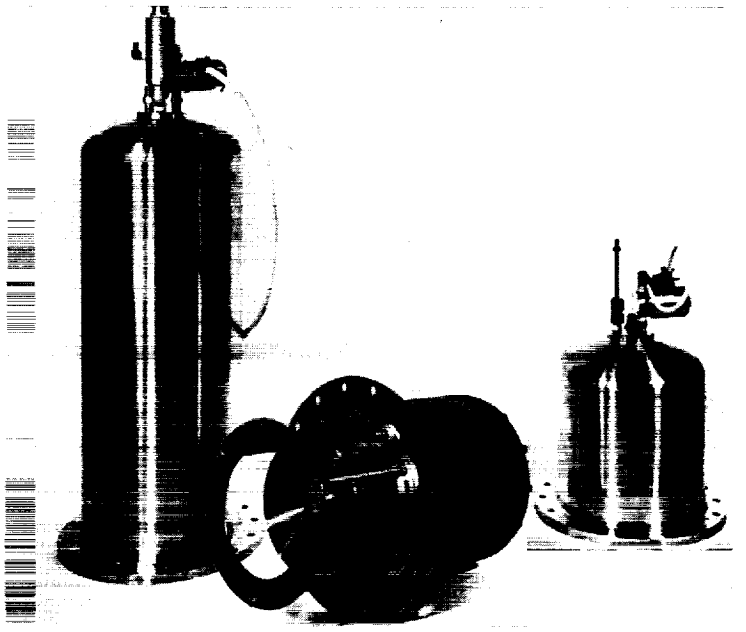

CS-40393

Figure II-41. - 500-Watt regenerative hydrogen-oxygen battery.

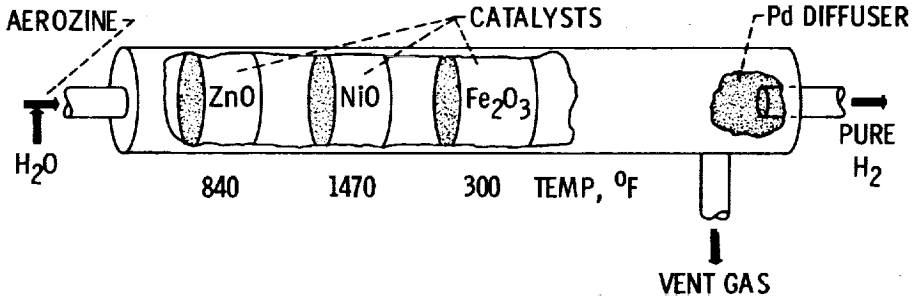

CS-40378

Figure II-42. - Aerozine 50 reformer. Typical product composition, mole percent: H_2, 40.4 (99.5-percent yield); N_2, 10.2; NH_3, 0.3; H_2O, 42.9; CO, 0.4; CO_2, 6.0; CH_4, <0.1.

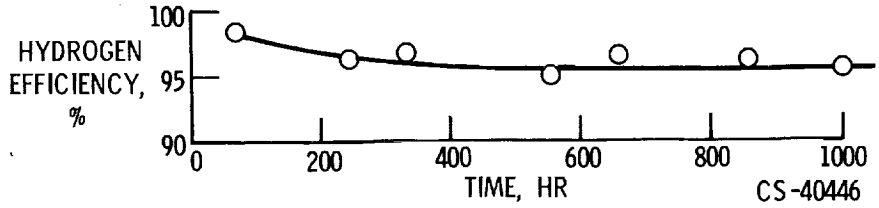

Figure II-43. - Life tests of Aerozine 50 reactors.

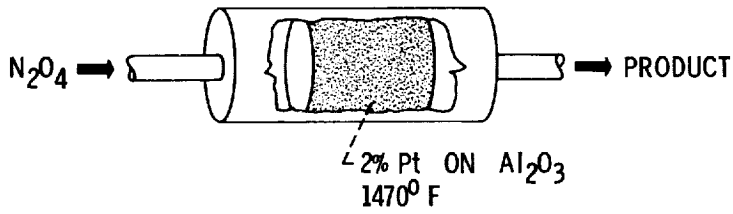

TYPICAL PERFORMANCE: $N_2O_4 \rightarrow N_2 + 2O_2$

TIME, HR	N_2O_4 CONVERTED, %
60	99
80	79
470	79
675	76
900	80
1000	79

CS-40376

Figure II-44. - N_2O_4 decomposition reactor.